AD-A047 224 SPERRY RESEARCH CENTER SUDBURY MASS F/G 20/6
MULTIPLEXING AND FILTERING OF OPTICAL SIGNALS.(U)
JUN 77 A R NELSON DAAB07-76-C-1343
UNCLASSIFIED SCRC-CR-77-40 ECOM-1343-F NL

1 OF 2
AD
A047224

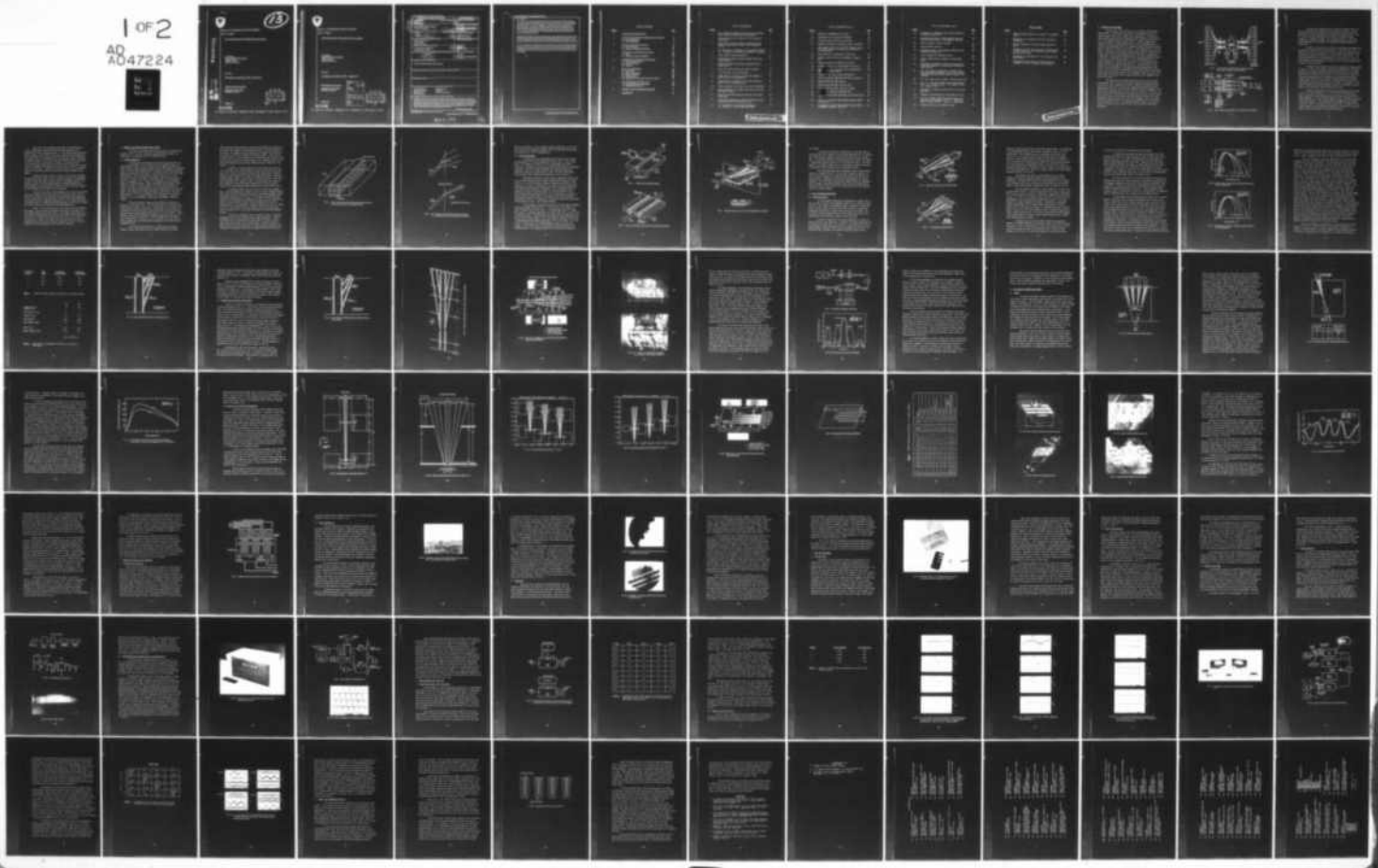

4722

1.0
1.1
1.25
1.4
1.6
2.8
2.5
3.2
2.2
3.6
2.0
4.0
1.8

MICROCOPY RESOLUTION TEST CHART
NATIONAL BUREAU OF STANDARDS 1963-A

AD A047224

AD No. ____
DDC FILE COPY

13
B.S.

Research and Development Technical Report

ECOM -76-1343-F

MULTIPLEXING AND FILTERING OF OPTICAL SIGNALS

A. R. Nelson
SPERRY RESEARCH CENTER
100 North Road
Sudbury, MA 01776

June 1977

Final Report for Period 29 April 1976 – 29 April 1977

DISTRIBUTION STATEMENT

Approved for public release;
distribution unlimited.

DDC
RECEIVED
DEC 5 1977
D

Prepared for:

ECOM

US ARMY ELECTRONICS COMMAND FORT MONMOUTH, NEW JERSEY 07703

Research and Development Technical Report

ECOM -76-1343-F

MULTIPLEXING AND FILTERING OF OPTICAL SIGNALS

A. R. Nelson
SPERRY RESEARCH CENTER
100 North Road
Sudbury, MA 01776

June 1977

Final Report for Period 29 April 1976 – 29 April 1977

ACCESSION for
NTIS White Section X
DDC Buff Section
UNANNOUNCED
JUSTIFICATION
BY
DISTRIBUTION/AVAILABILITY CODES
Dist. AVAIL. and/or SPECIAL
A

DISTRIBUTION STATEMENT

Approved for public release; distribution unlimited.

DDC
RECEIVED
DEC 5 1977
D

Prepared for:

ECOM

US ARMY ELECTRONICS COMMAND FORT MONMOUTH, NEW JERSEY 07703

SECURITY CLASSIFICATION OF THIS PAGE (When Data Entered)

REPORT DOCUMENTATION PAGE

READ INSTRUCTIONS BEFORE COMPLETING FORM

1. REPORT NUMBER: ECOM-1343-F	2. GOVT ACCESSION NO.
3. RECIPIENT'S CATALOG NUMBER	
4. TITLE (and Subtitle): MULTIPLEXING AND FILTERING OF OPTICAL SIGNALS	5. TYPE OF REPORT & PERIOD COVERED: Final Report, 29 April 1976 – 29 April 1977
6. PERFORMING ORG. REPORT NUMBER: SCRC – CR-77-40	
7. AUTHOR(s): Nelson, Arthur R. / Nelson	8. CONTRACT OR GRANT NUMBER(s): DAAB07-76-C-1343
9. PERFORMING ORGANIZATION NAME AND ADDRESS: Sperry Research Center, 100 North Road, Sudbury, MA 01776	10. PROGRAM ELEMENT, PROJECT, TASK AREA & WORK UNIT NUMBERS
11. CONTROLLING OFFICE NAME AND ADDRESS: U. S. Army Electronics Command, Fort Monmouth, NJ 07703	12. REPORT DATE: June 1977
	13. NUMBER OF PAGES: 90
14. MONITORING AGENCY NAME & ADDRESS (if different from Controlling Office): 99p.	15. SECURITY CLASS. (of this report): Unclassified
	15a. DECLASSIFICATION/DOWNGRADING SCHEDULE

16. DISTRIBUTION STATEMENT (of this Report)

Approved for public release; distribution unlimited.

17. DISTRIBUTION STATEMENT (of the abstract entered in Block 20, if different from Report)

18. SUPPLEMENTARY NOTES

19. KEY WORDS (Continue on reverse side if necessary and identify by block number)

Optical Multiplexing
Optical Demultiplexing
Multimode Fibers
Numerical Aperture
Throughput Losses
Bandwidth
Signal-to-Crosstalk Ratio

20. ABSTRACT (Continue on reverse side if necessary and identify by block number)

The objective of this contract is to develop an optical multiplexing device to combine onto one channel the information carried on several separate fiber optic channels and, subsequently, to perform the demultiplexing operation after transmission over distances of the order of a km. The main research effort is the development of the optical multiplexing/demultiplexing device. This device must be compatible with multimode fibers of relatively large numerical aperture, exhibit total throughput losses less then 15 dB, total signal to crosstalk ratio of more then 20 dB, and a bandwidth capability of 1.3 MHz.

(Continued on reverse side)

DD FORM 1 JAN 73 1473 EDITION OF 1 NOV 65 IS OBSOLETE

SECURITY CLASSIFICATION OF THIS PAGE (When Data Entered)

408 199

20. ABSTRACT

This report covers the work performed during a one year effort beginning May, 1976. During the past year a complete multiplexed optical data link that meets nearly all of the criteria outlined above has been constructed and tested. The main effort centered on the development of the actual electro-optic multiplexing device itself, a thin crystal of $LiTaO_3$ that controls the flow of light with the application of appropriate voltages. Several designs were constructed and tested before the final design was chosen. The final multiplexer design exhibited less that 15 dB throughput loss, and operates at high frequency with up to .25 numerical aperature fibers. The inherent signal to crosstalk ratio is about 15 dB, 5 dB less than the requested performance.

Following the construction of the devices, permanent fiber-to-device connections were developed, and the complete multiplexer and demultiplexer units were packaged with integral butt coupled fibers. This is the first reported development of an optical switch with fibers produced as a permanent package. All performance characteristics were maintained except for the signal to crosstalk ratio which declined to about 12 dB.

Finally, the multiplexer units and fibers were operated successfully in a complete multiplexed optical data link. A GaAlAs laser source was modulated at 32 kbit/s while the multiplexer and demultiplexer sampled each channel at the rate of 10 times per bit. The output was monitored by a PIN photodetector, and the total link loss for the multiplexer and demultiplexer units and a fiber-to-fiber connector was measured at less than 30 dB.

TABLE OF CONTENTS

LIST OF ILLUSTRATIONS

PRECEDING PAGE BLANK-NOT FILMED

LIST OF ILLUSTRATIONS (cont.)

LIST OF ILLUSTRATIONS (cont.)

LIST OF TABLES

PRECEDING PAGE BLANK-NOT FILMED

1. INTRODUCTION AND SUMMARY

The objective of this contract is to develop an optical multiplexing device to combine onto one channel the information carried on several separate fiber optic channels and, subsequently, to perform the demultiplexing operation after transmission over distances of the order of a km. The proposed system is shown in Fig. 1. Twelve transmitting stations use LED's or semiconductor lasers to send asynchronous data at 32 kbit/s over multimode fibers to a centrally located multiplexer station. Figure 2 shows this station in more detail. The information on the twelve fibers is combined by time division multiplexing (sampled at 320 kbit/s per channel) onto three fibers by means of three identical 4:1 multiplexers. In addition, a visible LED is modulated with the timing information, which is also sent on the multimode fibers. At the demultiplexing end, the timing information is separated by color filters, and identical optical devices perform the demultiplexing operation. The main thrust of this contract is the development of the optical mutliplexing/demultiplexing device. This device must be compatible with multimode fibers of relatively large numerical aperture, exhibit total throughput losses less than 15 dB, total signal to crosstalk ratio of more than 20 dB, and a bandwidth capability of 1.3 MHz.

This report covers the work performed during a one year effort beginning May 1976. During the past year a complete multiplexed optical data link that meets nearly all of the criteria outlined above has been constructed and tested. The main effort centered on the development of the electro-optic switching device, a thin crystal of $LiTaO_3$ that controls the flow of light with the application of appropriate voltages. Several designs were constructed and tested before the final design was chosen. The final multiplexer design exhibited less than 15 dB throughput loss, and operates at high frequency with up to .25 numerical aperture fibers. The inherent signal to crosstalk ratio is about 15 dB, 5 dB less than the requested performance.

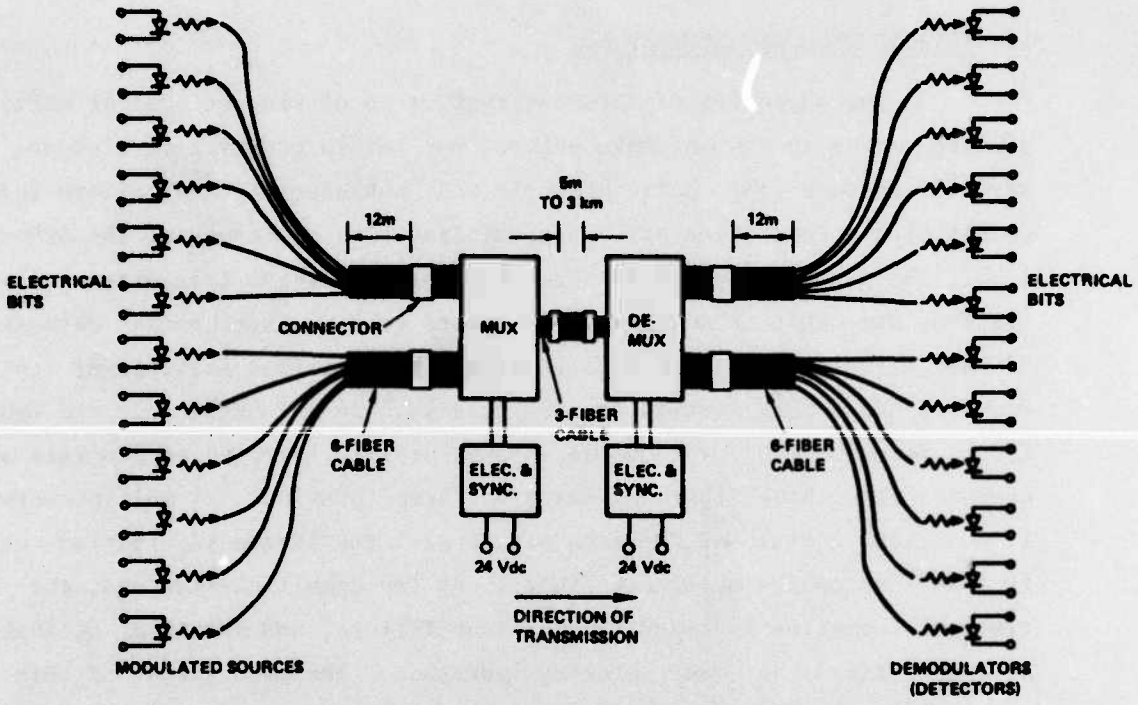

FIG. 1 Block diagram of complete optical data link employing electro-optic multiplexer and demultiplexer.

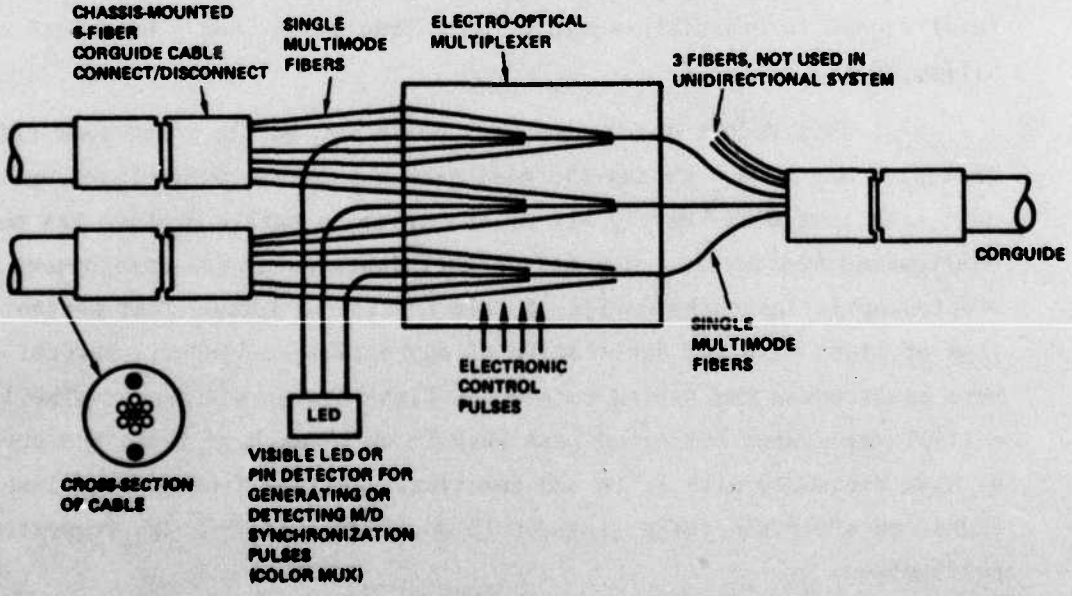

FIG. 2 Fiber connection block diagram for 3 dB coupler EO multiplexer.

Following the construction of the devices, permanent fiber-to-device connections were developed, and the complte multiplexer and demultiplexer units were packaged with integral butt coupled fibers. This is the first reported development of an optical switch with fibers produced as a permanent package. All performance characteristics were maintained except for the signal to crosstalk ratio which declined to about 12 dB.

Finally, the feasibility of optical multiplexing was demonstrated by operating the multiplexer units and fibers in an optical data link. A GaAlAs laser source was modulated at 32 kbits/s while the multiplexer and demultiplexer sampled each channel at the rate of 10 times per bit. The output was monitored by a PIN photodetector, and the total link loss for the multiplexer and demultiplexer units and a fiber-to-fiber connector was measured at less than 30 dB.

The next seven sections of this report describe the progress made in detail. In Sec. 2, the general principles of operation of the Sperry Research Center (SCRC) multimode optical switching devices are discussed. Electrodes are evaporated on both sides of a thin crystal of $LiTaO_3$, and an applied voltage across the thickness of the crystal produces index changes which direct the flow of light. Multimode fibers are directly butt coupled to the input and output of the crystal. In addition, a non-normal incidence butt coupling scheme can be used to collimate the fiber light so that relatively large NA fibers can be used.

Section 3 describes the first optical multiplexer design, known as the 3 dB coupler multiplexer. In this version of the multiplexer, light is guided in a main channel and may be switched into any of four branch channels by a control voltage applied to gate electrodes which guard the branch entrances. This design achieved throughput losses of about 15 dB and a signal to crosstalk ratio of only 10 dB. In addition, this version required a long crystal for fabrication, more than 7 cm, and this leads to some difficulties in the fabrication process.

Soon after the 3 dB coupler multiplexer was constructed and tested, a new design termed the spoiler electrode multiplexer was developed, and this is described in Sec. 4. The spoiler design allows the light to emanate freely from the input butt coupled fiber and impinge on four output ports at the opposite end of the crystal. Spoiler electrodes are placed in front of these output ports and block or open the entrances to the output fiber in response to a voltage. The spoiler design achieves throughput losses between 10 and 15 dB with a signal to crosstalk ratio of 14 to 16 dB. In addition it requires only a 3 to 4 cm length of $LiTaO_3$ for construction, about one-half that of the 3 dB coupler multiplexer.

Coupling of optical fibers is one of the more critical problems for most optical data links, and Sec. 5 details the results of packaging an electro-optic device with coupled fibers in a permanent fashion. The procedure entails creating accurate grooves photolithographically for fiber alignment and then epoxying the fibers in place. The fiber holders are then aligned with the device and also epoxied.

Section 6 describes the other components used in the test optical data link. Connectors are again required for source to fiber, fiber to detector, and fiber to fiber coupling. The multiplexer and demultiplexer drive electronics were developed specifically for this project and supply a sequential 400 V, 1.28 MHz signal while consuming less than 50 W of power. The source, detector, and fiber were purchased commercially.

In Sec. 7 the detailed results of the tests run on the packaged multiplexers and the complete multiplexed data link are described. No operational problems were noted; that is, the packaged devices functioned in the link as predicted from the optical bench tests. This entire link was delivered to ECOM, while another link was constructed for further experimentation at SCRC. The research is summarized in Sec. 8, and suggestions for future improvements and research are included.

2. THEORY OF MULTIMODE LAYERED OPTICAL DEVICES

The theory of multimode optical switching used by SCRC has been detailed in Ref. 1 and the references contained therein; however, for completeness the important points are summarized here.

2.1 General Background

A technique for creating active optical switching devices has been developed at SCRC. This technique uses the quadratic behavior of Snell's law for light incident at grazing angles onto boundaries containing small refractive index discontinuities to cause electrically controllable amounts of refraction or reflection. Using Snell's law in the small angle approximation, the critical angle for internal reflection θ_c can be expressed in terms of the index of the medium n and the index change Δn across the boundary as $\theta_c^2 = 2\Delta n/n$. The importance of this quadratic behavior is readily apparent. Namely, fractional index changes of 10^{-3} suffice to produce a critical angle of 1.7^o and hence enable one to reflect or to pass any beam having an angular divergence of less than this amount. The utility of the above observation stems from the fact that index changes of 10^{-3} can be produced electro-optically in a variety of materials, e.g., $Sr_{1-x}Ba_xNb_2O_6$, $KTa_xNb_{1-x}O_3$, $Ba_2NaNb_2O_{15}$, $LiTaO_3$ and $LiNbO_3$.

Of these materials, $LiNbO_3$ (LN) and $LiTaO_3$ (LT) appear most practical at the present time. The crystal growth art for LN and LT has become highly refined in recent years. Large boules 12 cm long and 5 cm in diameter with excellent optical quality and high resistivity are now grown routinely and are commercially available at costs of $\$9/cm^3$. These materials can be polished without introducing significant work strain, have a high Pockel's coefficient, a low loss tangent, are resistant to optical damage, and are stable against depoling over the entire military temperature range.

Given the materials LN and LT to work with, the principal design criteria, high input and output coupling efficiencies between

fibers and electro-optic material, can be met by choosing the thickness of the electro-optic medium to be approximately equal to the core diameter of the fibers. The simplest type of electro-optic multimode device that one may construct consists of a single electro-optic channel. Such a device is shown in Fig. 3. This structure uses the upper and lower surfaces of the crystal both to confine the injected light to the crystalline layer, and to create perpendicular electric fields through the entire thickness of the crystal.

Although it is readily apparent that the high index of LN or LT (~ 2.2 for both e and o rays) suffices to confine a highly divergent light beam to the crystal, such highly divergent light beams cannot be readily controlled in the plane of the crystal by electro-optic means. Using the structure shown in Fig. 3, an excitation of 400 volts across a 75 μm thick crystal produces a 10^{-3} change in index. As noted above, this change is only sufficient to guide light that diverges by $\pm 1.7^{\circ}$ in LT or LN or, because of the index change between crystal and air, about $\pm 3.8^{\circ}$ in air.

A potential problem then arises due to the fact that voltages much in excess of 400 must be avoided in order to prevent breakdown through the crystal and the fact that most multimode fibers have divergence angles appreciably greater than $\pm 4^{\circ}$ in air. A very simple technique has been developed for simultaneously collimating the light while butt coupling the light to the electro-optic crystal, thereby eliminating the need for external lenses. This collimation technique, illustrated in Fig. 4, allows the $\pm 7.5^{\circ}$ to $\pm 15^{\circ}$ emission angle of multimode fibers to be controlled electro-optically in LT or LN without exceeding the crystalline breakdown voltage.

In Fig. 4(a), divergent light is incident at angle θ from glass through air onto a crystal having an index greater than glass. Snell's law indicates that rays incident at larger angles are bent to a greater degree than rays incident at more normal angles. Figure 4(b) shows a natural extension of this idea where the intermediate air region has been eliminated by cutting the fiber end at an angle and directly butting the

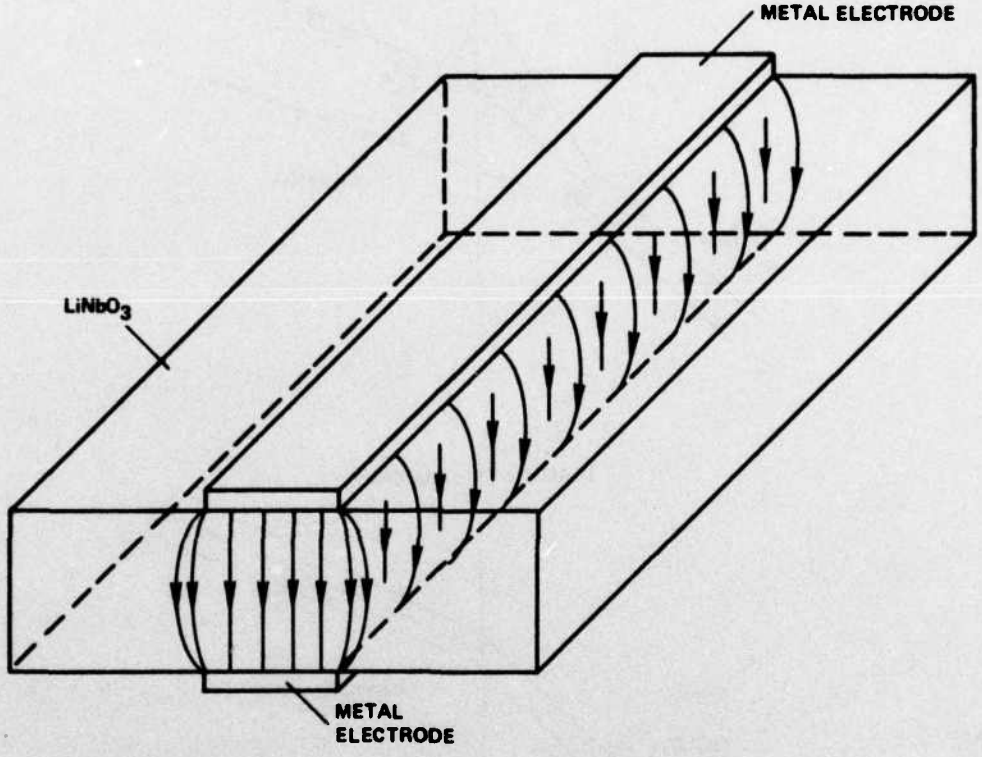

FIG. 3 Electro-optic channel produced by applying voltage across an electro-optic crystal such as $LiNbO_3$ or $LiTaO_3$.

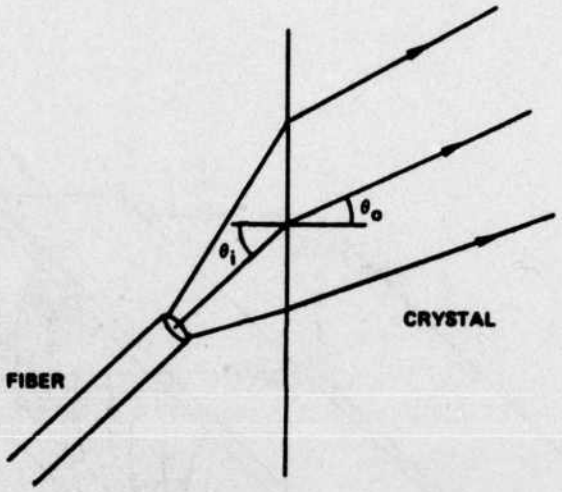

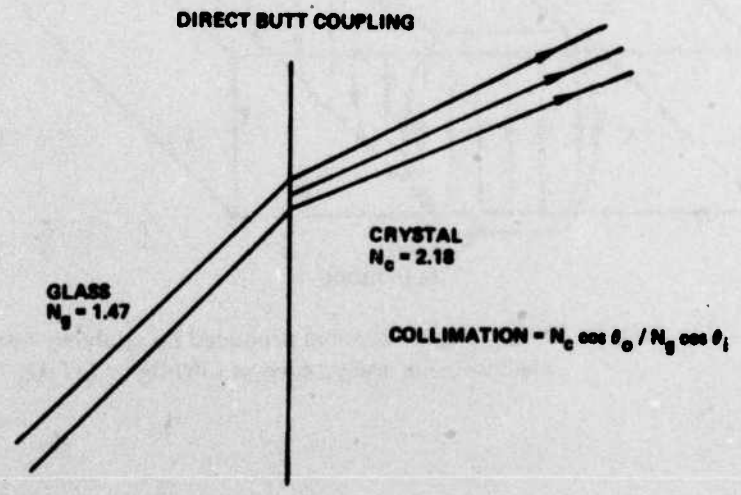

FIG. 4 (a) Principle of collimation via non-normal incidence.
(b) Collimation by non-normal incidence butt coupling.

fiber to the crystal. One can readily show for a glass-LT (or LN) interface that fibers terminating at angles of 69°, 75° and 79° yield collimation factors of 2, 3 and 4, respectively.[1]

2.2 Device Applications

By controlling the effectiveness of the electro-optic channel, one can construct the two port modulator[2] shown in Fig. 5. This device uses a 75 μm thick c-cut wafer of LT 1.5 cm long with Cr/Al stripe electrodes. Although the insertion loss from a Corning fiber is relatively large due to the use of normal-incidence butt coupling, 50% and 25% modulation depths were induced with 15 V and 5 V ac rms, respectively. The rise time of this modulator was measured to be less than 3 ns.

Additional improvements in the design of modulators of this type were recently obtained using the double strip-electrode geometry[3] shown in Fig. 6. For this structure a voltage is applied to two pairs of electrodes so as to produce a decrease in n on either side of the light path. This method yeilds equivalent performance as far as modulation depth is concerned, but may be superior because: (1) "barrier guides" do not suffer from electrode absorption loss,[1] (2) the light does not travel in the high electric field region of the crystal, thus limiting possible photoelectric effects, (3) light that is outside the guide can be prevented from entering the guide, thus limiting crosstalk.

The next device fabricated at SCRC was the electrically controlled directional coupler[4] shown in Fig. 7. In this case a 54 μm thick c-cut plate of single crystal LN was used. The branch angle lies at 1° angle with respect to the main channel and has a width that tapers to zero in the interaction region. The gap between the branch and main channels was 75 μm and the total crystal length 1.7 cm. The switch was designed to work with a light beam having an angular divergence of ±2° in the crystal (i.e., ±4° in air) for which case the 1° branch geometry creates an active 3 dB coupler. LN was chosen because the dielectric anisotropy enlarges the lateral spread of the fringing fields into the interelectrode region of

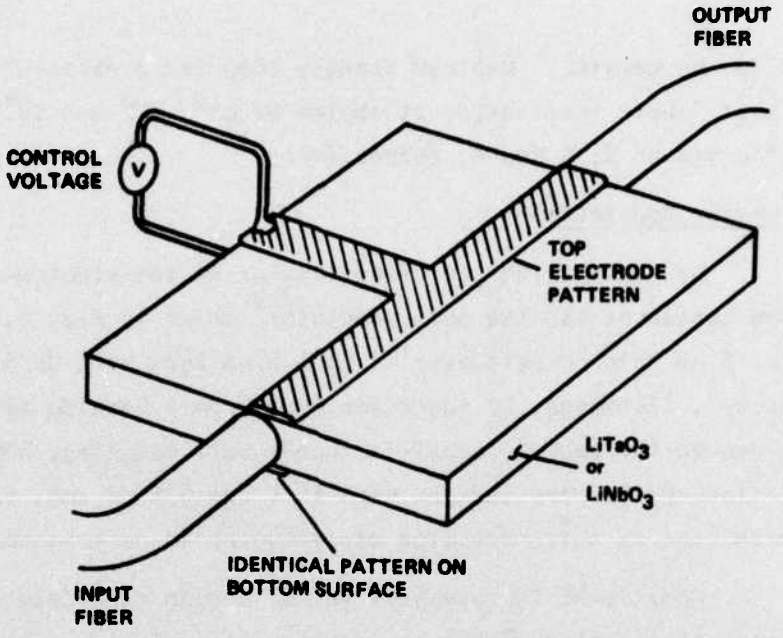

FIG. 5 $LiTaO_3$ channel waveguide modulator.

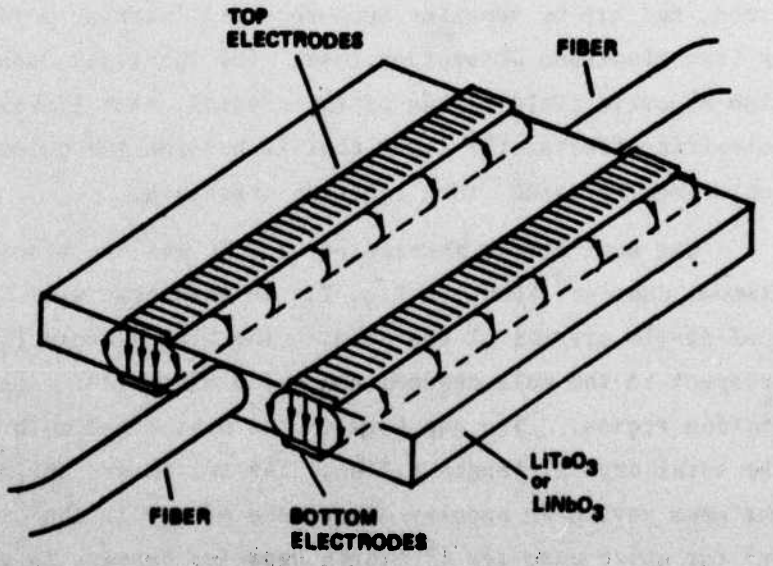

FIG. 6 Electro-optic channels created by double strip electrode geometry.

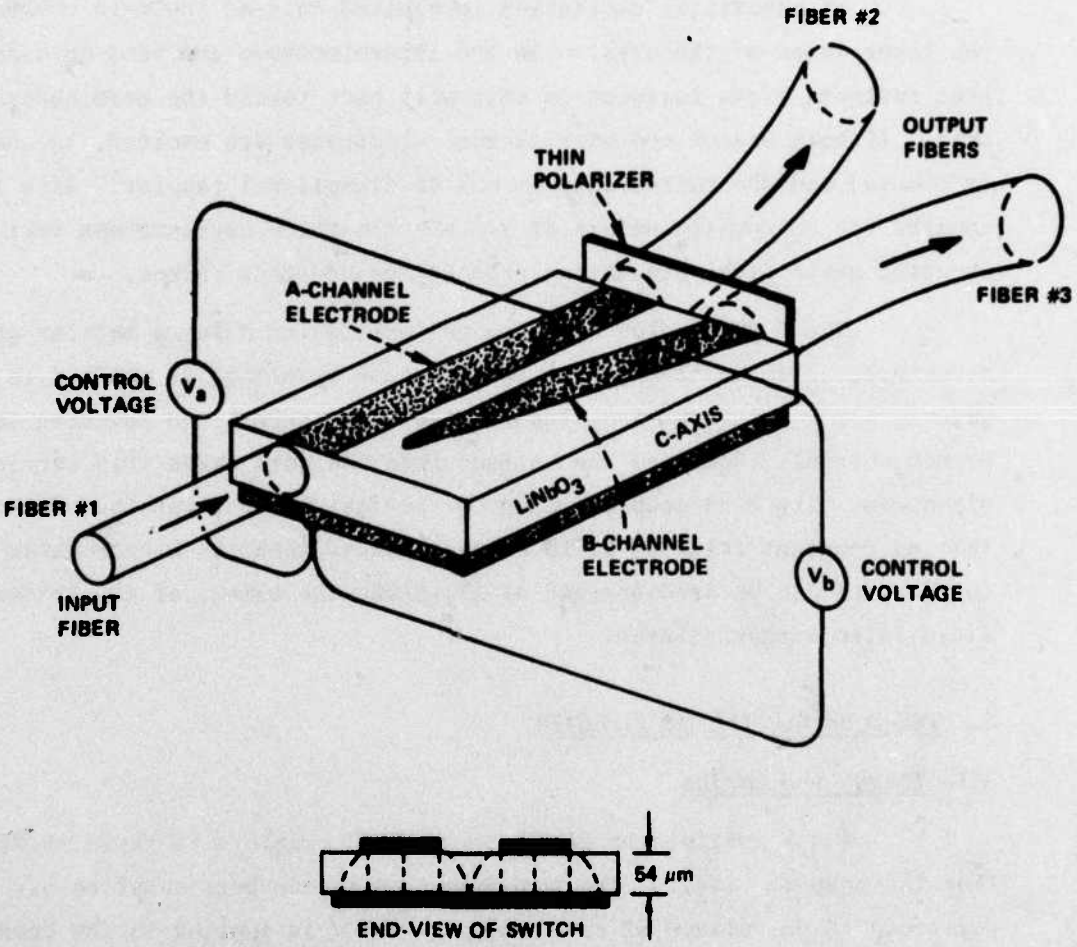

FIG. 7 Schematic diagram of three-port multimode electro-optic switch.

the crystal.

If electrical excitation is applied only to the main channel, the lower index of the crystal in the interelectrode gap acts as a barrier that reflects light incident on this wall back toward the main channel axis. If both branch and main channel electrodes are excited, the barrier is removed and the switch acts as a 3 dB directional coupler. With this coupler the achromatic nature of the electro-optic barriers was verified by using white light excitation from an incandescent source.

The 3 dB coupler may also be implemented using a barrier guide structure, as shown in Fig. 8. In this case a voltage is applied to a gate to block the light from leaving the main channel and entering the branch channel. Removing the voltage from the gate makes this barrier disappear. The 3 dB coupler using barrier guides thus has the advantage that no remanent fringing field barrier exists when the branch guide is open and LT can be used instead of LN, since the extent of the fringing field is no longer relevant.

3. THE 3 dB COUPLER MULTIPLEXER

3.1 Theory and Design

A 4:1 multiplexer design using 3 dB couplers is shown in Fig. 9. (For the sake of clarity, the non-normal incidence butt coupling has been omitted.) A dc voltage of approximately 400 V is applied to the barrier guide electrodes, while the time division multiplexing is performed by sequentially removing the voltages from the four gate electrodes. The reciprocity theorem guarantees that the same device can be used for demultiplexing by reversing the direction of the light flow.

In order to design the 3 dB coupler multiplexer, the fiber NA and core size are first specified. In general, this NA may range from .14 to .30, while the core diam is 50 to 85 μm. As described in Sec. 2, the maximum angular range of TM light that may be guided is less than $\pm 2^{o}$ in the crystal and, therefore, the required collimation factor must be

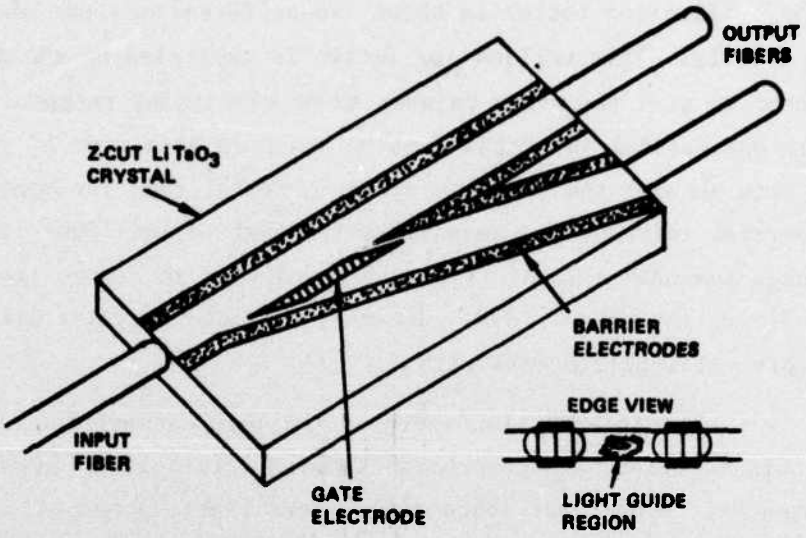

FIG. 8 Basic 3 dB coupler design using barrier guides.

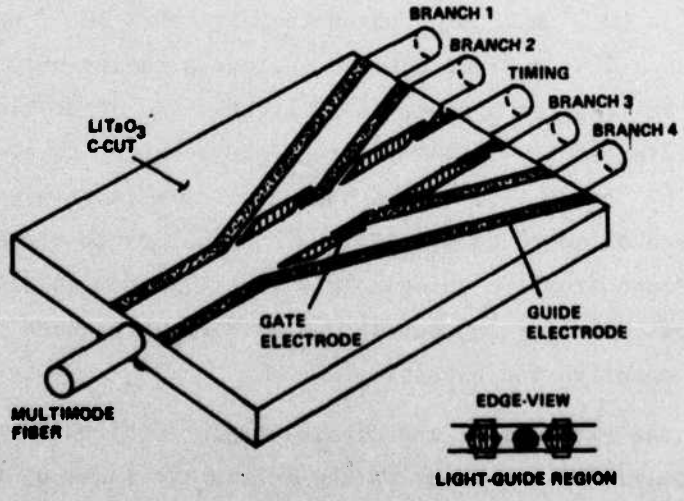

FIG. 9 4:1 multiplexer using 3 dB couplers.

computed to reduce the given NA to within that angular range. The magnitude of the collimation factor is about two-or three-fold for NA= .16 or .25, respectively. This collimation factor is multipled by the fiber core diameter to give the width between guide electrodes except that approximately one crystal thickness must be added on each side of the channel to take into account the fringing electric field[1] from the opposing electrodes. The crystal thickness is approximately equal to the fiber core diameter, although somewhat thinner crystals may be used to reduce the voltage without sacrificing throughput loss. However, a thinner crystal will be more fragile and more difficult to work with.

The intersection angle of the main channel and the branch channels is fixed by a compromise between interaction length and light throughput. A narrower angle yields more light tapped off, but the length of the coupler is given by the width of the branch divided by the tap-off angle, so that overall length considerations limit the angle to 1^{o} or so.

The 3 dB coupler multiplexer is also designed to use some of the TE light from the fiber. TE light is polarized in the plane of the crystal and, for z-cut LN or LT crystals, the appropriate electro-optic coefficient is $r_{13} = 7 \times 10^{-12}$ m/V, as opposed to $r_{33} = 30 \times 10^{-12}$ m/V used for the TM polarization. Thus a given applied voltage produces only 1/4 the index change for TE light as opposed to TM light. The quadratic relationship between guiding angle and the induced index change, however, actually allows 1/2 of the TE light to be guided. An introductory length of barrier guide is used on the 3 dB coupler design in order to allow the unguided TE light to escape from the guide. This light is then shielded from impinging on the output ports by the barrier guide structure which prevents outside light from entering the channel.

The exact fiber and crystal angle required for a particular degree of collimation depends on the refractive index of the fiber core and the crystal. Since the angular cone of light to be controlled is only $\pm 2^{o}$, clearly the angular tolerance for matching the fiber to the electrode pattern on the crystal is critical and therefore the refractive indices

of fiber and crystal must be determined quite accurately.

The fiber core index was determined by etching off the fiber cladding with buffered HF, and then using a series of known index fluids with the fiber core. The fiber core was immersed in this sequence of fluids and photographed under a microscope. When the fiber core index fluid interface vanished, the fiber core index equalled the fluid index. This occurred for n=1.465 for λ=.589 μm for the Corning fiber, which extrapolates to n=1.464 at λ=.633 μm if the dispersion curve for pure fused silica[5] is used. Note that this result is not the same as the refractive index for pure fused silica, which is n=1.457 at .63 μm.

The crystal index for LT can vary considerably depending on the composition of the melt.[6] The LT used for the multiplexer was grown from the congruent composition[7] (LiTa=.951), which implies a refractive index of n_e=2.182. In order to confirm this, measurements were made using the method of minimum deviation and a prism of LT. These experiments gave n_e=2.177, which is considerably off from the predicted value. A compromise value of 2.180 was used in the calculations of collimation angle.

The exact angle of the electrode pattern relative to the crystal edge is also affected by the shape of the angular cone of light in the crystal. While the refractive index change will contain about $\pm 2^o$ in the crystal, when extreme angles are used for collimation, the actual cone of light is not symmetrical about the central ray. This comes about because the collimation and reflection coefficient are strong functions of the incident angle. A computer program was developed to compute the actual intensity profile of the fiber cone of light in the crystal and the results are shown in Figs. 10 and 11 for three-fold collimation and TM and TE polarizations, respectively. The graphs give light intensity vs the angle in the crystal relative to the central angle of 40.6^o computed[1] for three-fold collimation using the fiber and crystal indices given above. As can be seen from the graph, there is not a symmetrical cone of light, but rather a curve skewed toward smaller angles, especially for larger numerical aperture.

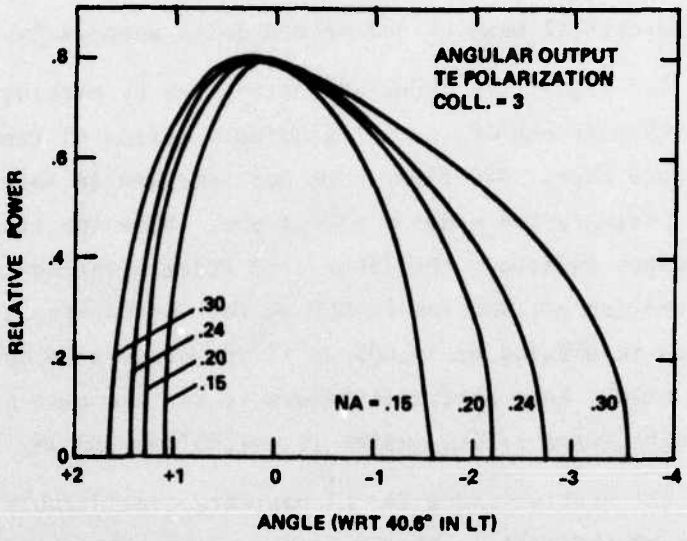

FIG. 10 Output power as a function of angle with respect to 40.6° in LT for TE polarization.

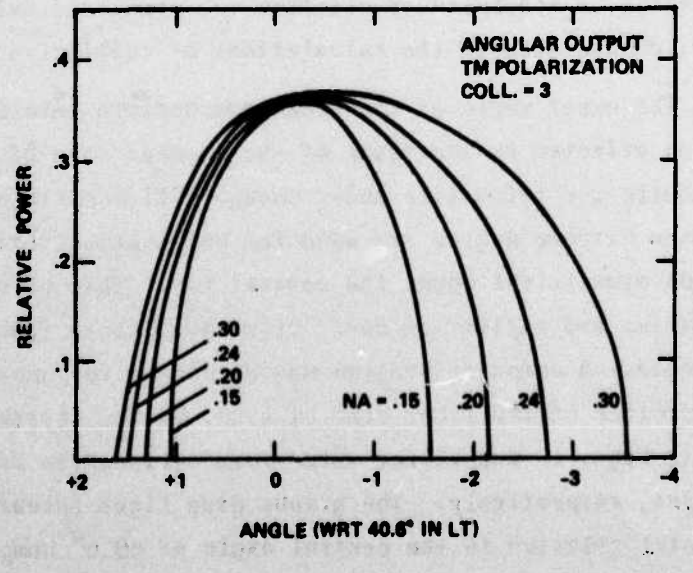

FIG. 11 Output power as a function of angle with respect to 40.6° in LT for TM polarization.

Therefore in computing the proper angle of the electrode pattern, a correction factor of $.6^{o}$ or $.4^{o}$ was used for three-fold or two-fold collimation, respectively. Table 1 summarizes the results of these calculations for NA $\geq$ .20.

There are a number of different contributions to the theoretical throughput loss for this multiplexer. The reflection losses for TE and TM light are 1 and 4.5 dB, respectively, for both interfaces using three-fold collimation. An index fluid can be used to cut this loss a great deal since, for n_g=1.47 and n_c=2.18, the optimum index for an antireflection layer is 1.62 at an incident angle of 75^{o}. This reduces the reflection losses to .5 and 2.5 dB for TE and TM light, respectively. Another loss occurs due to the portion of TE light which is not confined by the waveguide. Also, the light that is captured is free to spread in the fringing electric field to a width greater than the initial channel width, and this light is not recaptured, leading to an estimated 1 dB loss. Finally, there is a size and shape mismatch which is inevitable between the crystal and fiber, and this results in approximately 1.5 dB loss. These losses are shown in Table 2, and the total estimated loss is about 6 dB in going through the main channel. To this loss the switch loss must be added in order to obtain the output of the branch channel. A more detailed analysis of the switch loss should take into account the fringing electric field distribution, particularly in the region of the branch intersection. Such a numerical analysis has not been completed but a qualitative argument can be made which leads to the conclusion that there will be a 5 or 6 dB (TM) switching loss. Thus the total theoretical loss of this multiplexer is approximately 13 dB. There is also the possibility of decreasing this switch loss by inserting deflector electrodes in the main channel to tap off more of the light. However, this change would entail complicated electrical connections and would be difficult to fabricate at the present time.

There are a number of variations to the basic multiplexer design of Fig. 9. In Fig. 12, one of the four 3 dB couplers is shown with a "spoiler" electrode added to the branch channel, and electrically connected to the gate. The purpose of this electrode is to increase the signal to

Collimation Factor	Fiber Angle	Predicted Crystal Angle	Corrected Crystal Angle
2	66.9	38.2	37.8
3	75.3	40.6	40.0
4	79.2	41.3	40.5

Table 1. Fiber and crystal angles as a function of collimation factor.

	TE	TM
Reflection Loss (index fluid)	.5	2.5
Unconfined TE light	3.0	0
Fringing field	1.5	1.5
Size mismatch	1.5	1.5
MAIN CHANNEL OUTPUT	6.5	5.5
Switch Loss	9	6
BRANCH CHANNEL OUTPUT	15.5	11.5

AVG = 13 dB Loss

TABLE 2. Theoretical Loss Components in dB for the 3 dB Coupler Multiplexer.

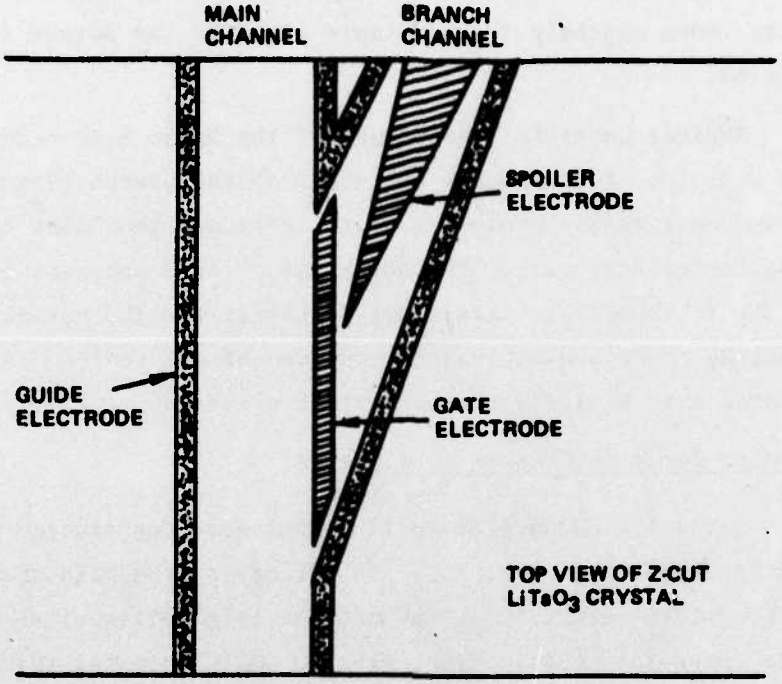

FIG. 12 Barrier waveguide 3 dB coupler with spoiler electrode.

crosstalk ratio by deflecting light which may leak through the gate when the branch channel is "off". In addition, a voltage applied to increase the refractive index may help to guide more light to the output fiber when the branch is on.

Another possible improvement of the basic 3 dB coupler design is shown in Fig. 13. In this case the width of the branch channels is tapered. This is a decollimation procedure which increases the light cone angle while shrinking the channel size. The advantage of this approach is that it may be possible to substitute this taper technique for the non-normal incidence butt coupling procedure at least at one end of the device. Also included in this design is a narrow stripe spoiler electrode.

3.2 Results for 3 dB Coupler Multiplexer

Several 3 dB coupler multiplexers were constructed using the guidelines outlined above in Sec. 3.1. In all cases, the main channel was 355 μm wide. This width results from the angular termination of an 85 μm core fiber for three-fold collimation, plus 50 μm (LT crystal thickness) added to each side for the fringing field. A branch angle of 1^{0} was used which implied a switch length of about 2.25 cm (switch length = channel width/$\sin(1^{0})$). Also, another 2.25 cm is used for the initial channel length, yielding a total device length of 6.75 cm. A sketch of the actual mask design is shown in Fig. 14. The drawing has an approximate 10:1 scale ratio so that the narrow branch angles are more visible. For this top mask, the electrical connections to the gate electrodes are brought out to the side of the crystal. The bottom mask is almost identical, except that the gate and barrier electrodes are connected and the pattern is at a uniform ground potential. Figure 15 illustrates the device in use with fibers and shows sections of the actual mask used to make the pattern of Fig. 9. Two photographs of a completed 4:1, 3 dB coupler multiplexer are shown in Fig. 16.

Two fibers were used for the testing: Corning (85 μm core, NA = .18) and ITT (50 μm core, NA = .25). In each case the He-Ne laser was used with two microscope objectives, 10x and 45x, so as to overfill the specified NA of both fibers. This resulted in a measured NA of .20

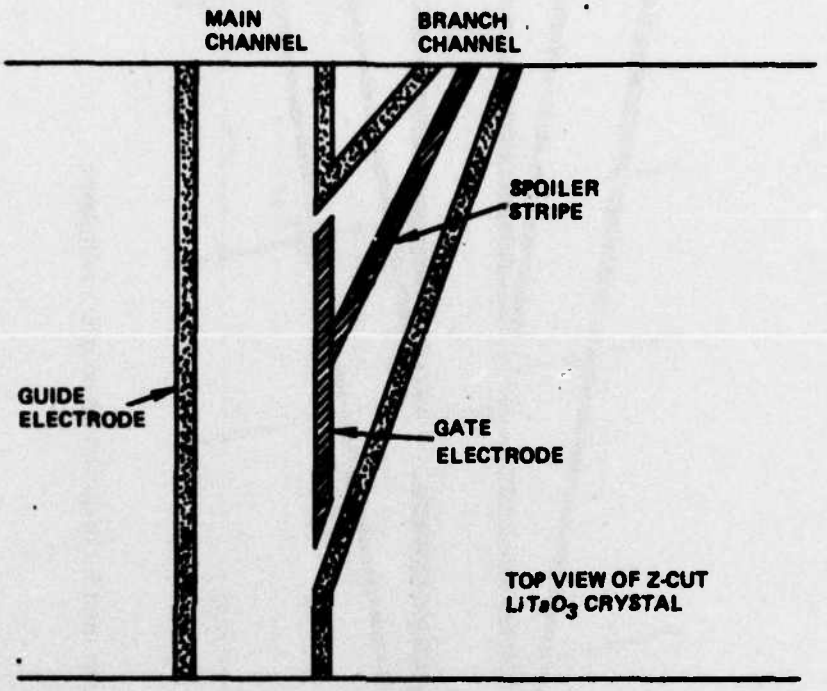

FIG. 13 Barrier waveguide 3 dB coupler with spoiler electrode and tapered output.

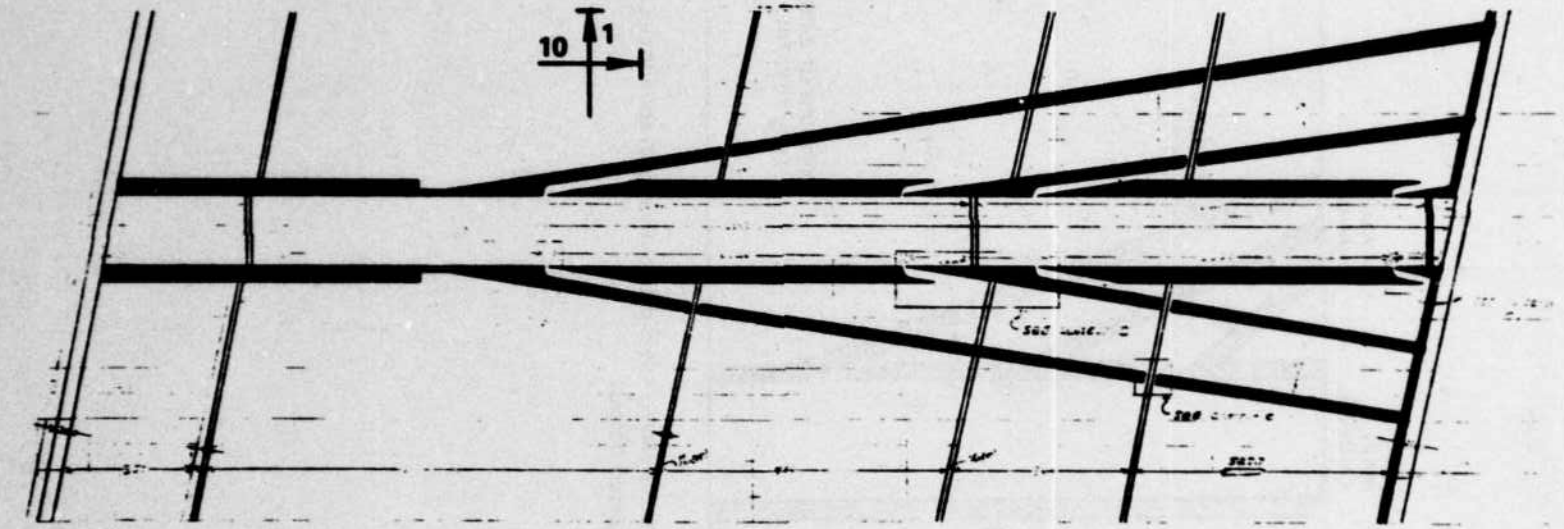

FIG. 14 Sketch of mask design used for original 3 dB coupler multiplexer.

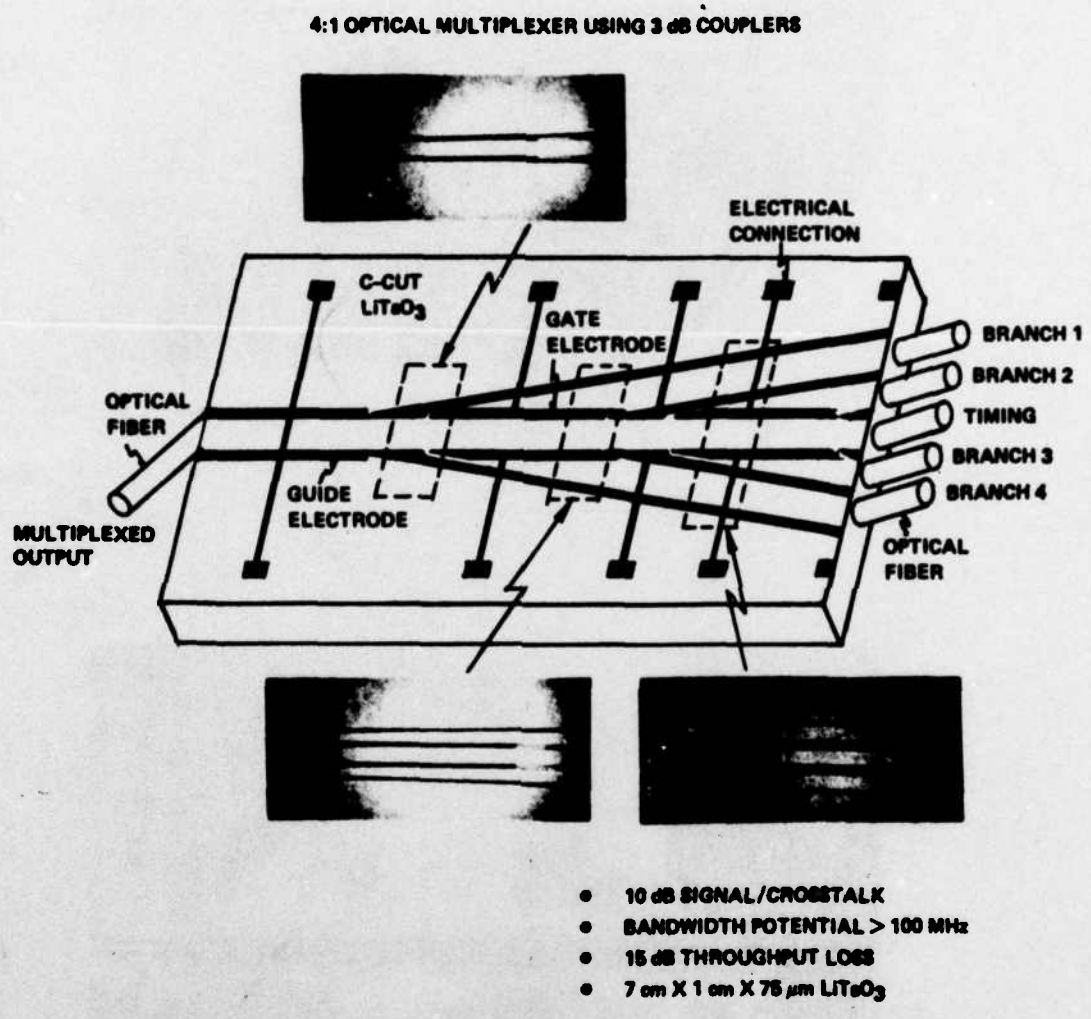

FIG. 15 3 dB coupler multiplexer in use with fibers and illustrated with photos of photoresist mask.

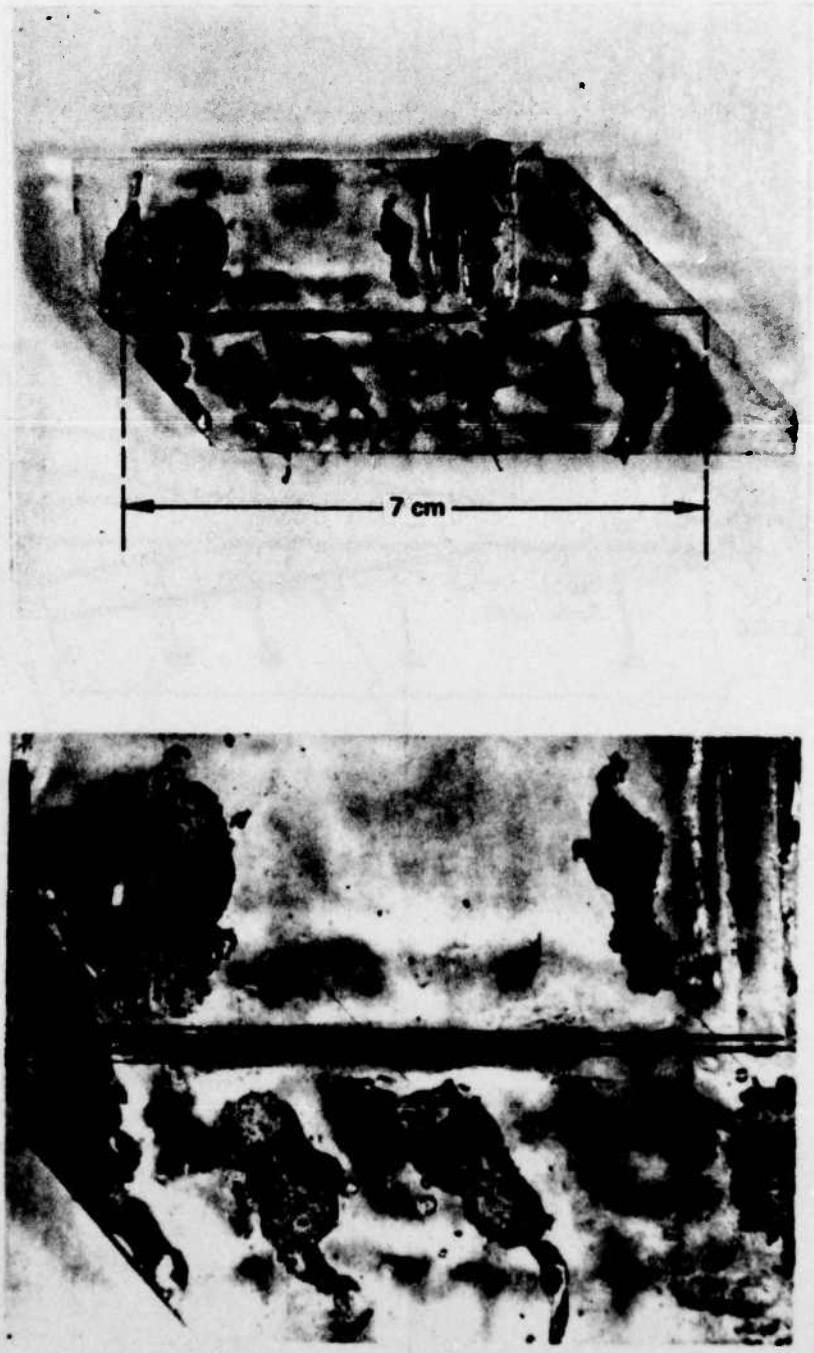

FIG. 16 (a) Overview of a 3 dB coupler multiplexer.
(b) Closeup of a 3 dB coupler multiplexer.

for the Corning fiber and .25 for the ITT fiber. The input and output lengths of fiber were about .5 m long with three-fold collimation terminations on one end. The values of throughput loss for the multiplexer which were measured are defined as the ratio of the power out of the input fiber divided by the power out of the output fiber. The experimental setup is shown in Fig. 17.

The basic performance of the 3 dB coupler multiplexer without spoiler electrodes is presented in the graph in Fig. 18. In this case the .25 NA fiber was used with the 4:1 multiplerer. +300 V was applied to the guide electrodes while the gates were switched between +300 V (closed) and -100 V (open). The output fiber was scanned along the output end of the crystal with one gate open for each run. From the graph we see that the output of the main channel is about 7 dB down from the input level. This is one dB more than the theoretical analysis predicts and might be due to imperfections such as slight misalignment of the fiber and crystal, or our loss estimates for the fringing field and size mismatch may be too optimistic. The output from the branch channels is 7 to 9 dB below the main channel intensity, which corresponds to the 7.5 dB predicted in Sec. 3.1. The total throughput loss is approximately 15 dB, which meets the minimum ECOM requirement.

The signal to crosstalk ratio defined as the output of the branch channel with the gate (open) divided by the gate (closed) output, can be read from the graph and in all cases is larger than 10 dB. Since this signal to crosstalk ratio was not felt to be adequate, two additional devices were built using the design of Figs. 12 and 13, which incorporate spoiler electrodes in the branch channels in order to improve the isolation of the output ports. Both devices had dimensions which were basically identical to the original design of Fig. 9, except that some modifications in construction were necessary in order to make electrical connections to the spoiler electrodes. In the standard design all electrical connections were brought out to the side of the crystal as shown in Fig. 14.

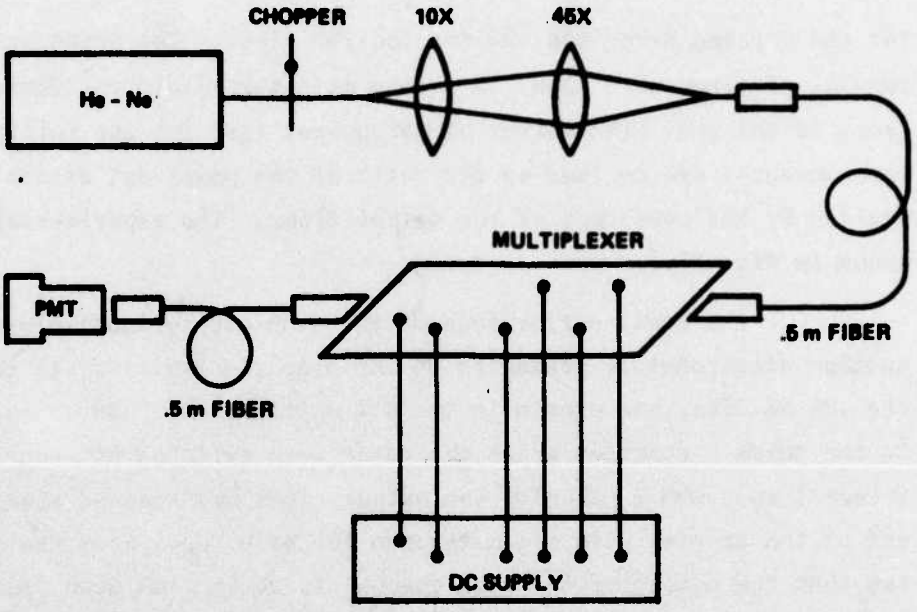

FIG. 17 Schematic of experimental test setup.

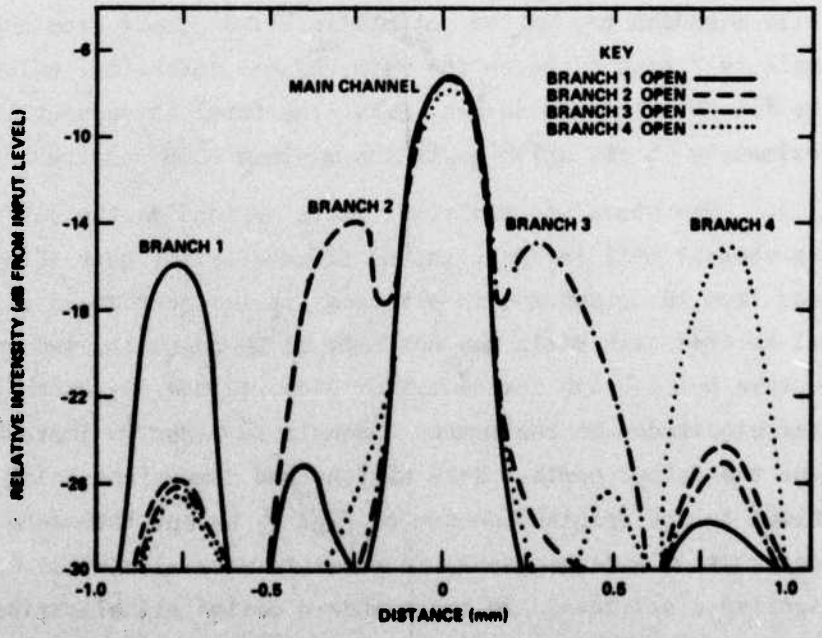

FIG. 18 Performance of 3 dB coupler multiplexer.

However, because of the complexity of the 3 dB coupler multiplexer with spoilers, electrical connections had to be made from above, through holes in an insulating layer of photoresist.

The initial measurements on the device with triangle spoilers indicated a small, perhaps 3 dB, improvement in the signal to crosstalk ratio. However, these initial measurements could not be reproduced, and a careful inspection showed that a crack had developed across the crystal producing an electrical open circuit for part of the electrical pattern and caused much scattered light. The thin, 50 to 75 μm crystals are quite fragile and care must be taken during various stages of construction. But after most devices are fabricated, they are sandwiched between glass plates and layers of glycolphthalate[1] making them generally quite secure and stable. It is possible that the added construction procedure required to make contact with the spoiler electrodes caused excess stress which led to the destruction of the device.

The second spoiler design used with the 3 dB coupler multiplexer employed a single stripe spoiler with tapered output ports. This device never operated properly and had a worse signal to crosstalk ratio than the standard design. The exact reason for this failure is not known, but again the stress caused by epoxying directly to the crystal in the region of light travel may have played a major role. Such mechanical stresses could cause imperfections in the crystal or induce refractive index changes capable of scattering the incident light. Theoretically, however, this design still seems promising, and improved fabrication techniques could overcome the above-mentioned difficulties.

An inherent drawback in a device design that requires construction on a crystal 7 cm by 50 μm thick is that the design will be difficult and expensive to implement. This difficulty also limits construction of several versions or iterations of similar device designs or even to fabricate multiple copies of a single design. This makes it difficult to perform the necessary experiments to maximize device performance. As

described above, three multiplexers were made, and one operated adequately, but further effort with this approach was not attempted due to the large size of the thin crystals. Therefore, an effort was made to find a design with at least equivalent performance, but using smaller crystals. The results using the new design are described in the next section.

4. THE SPOILER ELECTRODE MULTIPLEXER

4.1 Theory

The spoiler multiplexer design performs 4:1 multiplexing on an LT crystal of length significantly less than the 7 cm required for the 3 dB coupler multiplexer. This new design is shown (without butt coupling collimation, for simplicity) in Fig. 19. For this device, the light is allowed to spread freely from the butt coupled fiber and impinge on four output ports placed symmetrically at the opposite end of the crystal. A long narrow electrode is positioned in front of each output fiber, so that a decrease in refractive index will block the exit port, while reversing the voltage will help guide light to the output. In this design there is a minimum 6 dB power division loss, since the power is split among the four output ports, whereas in the 3 dB coupler design there is an inherent minimum 3 dB loss. However, as will be shown later, the total throughput loss is actually the same or lower for the new design.

One possible design procedure will now be outlined for the spoiler multiplexer. First, the size of the fiber core and the desired spacing between output ports (due to fiber cladding, for example) are specified and used to compute W, the overall width of the output section. Next, the fiber NA is used to calculate α, the maximum angle in the crystal, the crystal length L is fixed by the requirement that the cone angle fully illuminate W. The maximum angular range of light ϕ (Fig.20)

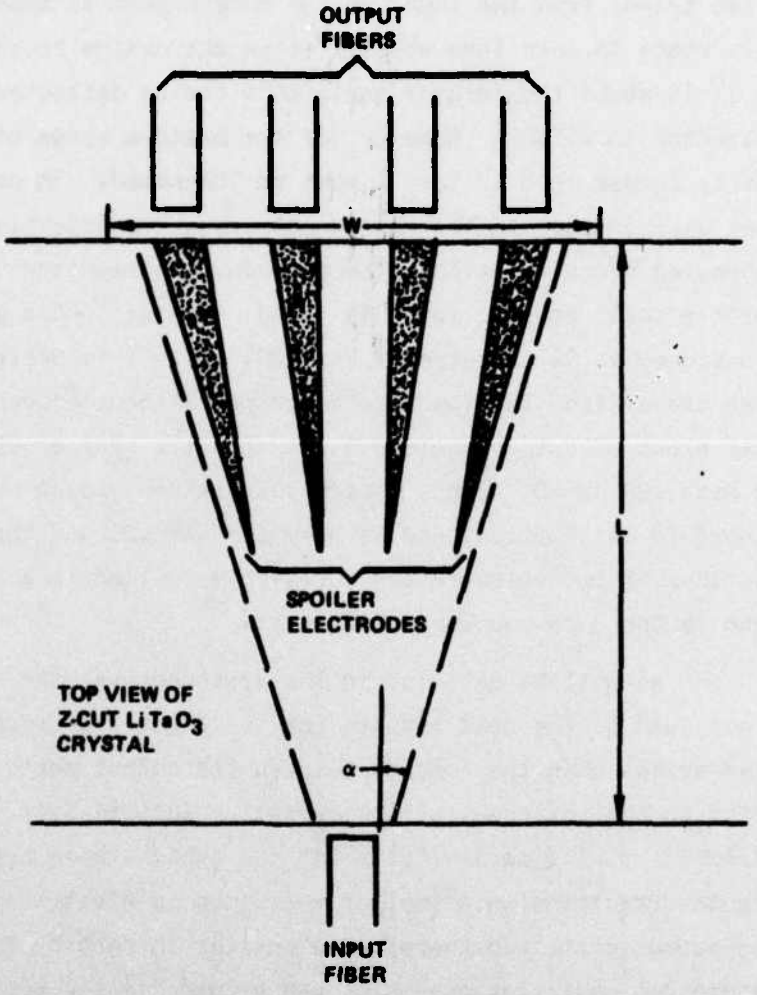

FIG. 19 Electrode design for spoiler multiplexer.

that can travel from the input to the output port is then computed. If this range is less than about 1^{o} then the design is satisfactory, since 1^{o} is about the largest angle that can be deflected for the TE polarization in $LiTaO_3$. However, if the maximum range of incident angles is larger than 1^{o} then L must be increased. In order to do this without also increasing the throughput loss, the effective fiber NA is decreased by collimation. The procedure is repeated until an acceptably small angular range is found. The deflector electrodes are then designed as illustrated in Fig. 20. With this design, no light ray can travel from the input to an output without encountering a spoiler electrode at an angle of less than 1^{o}. For an 85 μm core diam fiber with 125 μm OD, such a design calculation yields L=2 cm for NA= .17 and two-fold collimation, and L= 3 cm for NA= .25 and three-fold collimation. Thus, this device, using three-fold collimation, is about one-half as long as the 3 dB coupler multiplexer.

As will be detailed in the next section, the above procedure does not lead to the best results for the signal to crosstalk ratio. A problem arises when the spacing between the output ports becomes small relative to the thickness of the crystal. In this case, the fringing electric field will partly "fill in" the gaps between the spoiler electrodes resulting in a smaller variation in electric field intensity at the output ports and therefore a smaller Δn seen by the light rays. There are two modifications which can be made to the above basic design of Figs. 19 and 20 to remedy this situation: the electrodes can be made narrower and therefore cover a smaller output port, or the fibers can be separated by a larger distance. If the fibers are separated by a larger distance, then the crystal must be made longer in order that the angular cone will still fully illuminate the four outputs, and this will increase the throughput loss somewhat. In actual practice the optimum design was found by experimenting with several designs similar in structure to Fig. 19, but using various length and width modifications

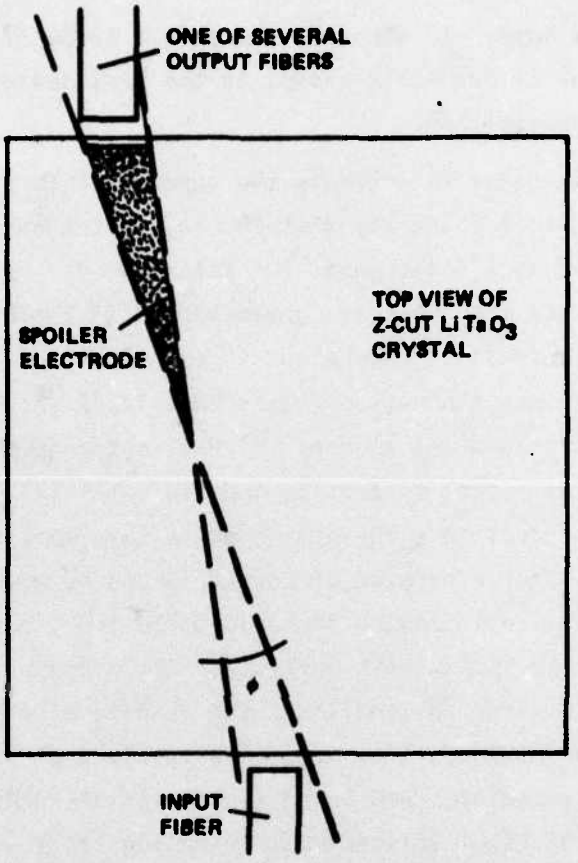

d_{core} = 85 μm		d_{fiber} = 125 μm
L (cm)	NA	COLLIMATION
1	.08	NONE
2	.17	2:1
3	.25	3:1

FIG. 20 Geometric procedure for designing spoiler electrodes.

as discussed here. In general, there is a tradeoff of throughput loss versus signal to crosstalk ratio, so the best device will depend on the particular application.

In order to estimate the throughput loss for the spoiler multiplexer, the light intensity distribution at the output end of the crystal must be known as a function of the fiber and device parameters. There are several factors that must be considered: (1) The circular cone of the fiber in free space is compressed in one dimension by the $LiTaO_3$ wafer; (2) The fiber has a non-zero width; that is, light cannot be considered to emanate from a point source; (3) Rays entering the crystal at different angles have different reflection coefficients; (4) The collimation procedure tends to collimate the higher angle rays more than the lower angle rays. The computer program of Section 3 can be modified to perform this calculation. The following are adjustable input parameters: fiber diameter fiber NA, fiber index, anti-reflection fluid index, crystal index, crystal length, and desired collimation. The results of a typical calculation are given in Fig. 21 for 3.5 cm long $LiTaO_3$, using an 85 μm fiber with NA= .25, three-fold collimation and an AR fluid with n= 1.62. As can be seen from the graph, the light intensity distribution at the output end of the crystal is far from uniform.

The non-uniform light distribution means that the throughput loss will depend on where the output ports are positioned and will be different for each port. The loss can be found by computing the light power in the area occupied by the output fiber, dividing by the total input power, and adding one to two dB extra loss for size mismatch of the fiber and crystal. For the three-fold collimation case, we find that the total theoretical loss ranges from 11 to 13 dB for the four output fibers. If the roles of the inner and outer branches of the multiplexer are reversed for the demultiplexer, then the maximum loss will decrease to the average of the best and worst case loss, or about 12 dB. Furthermore, this throughput does not include any increase in light intensity

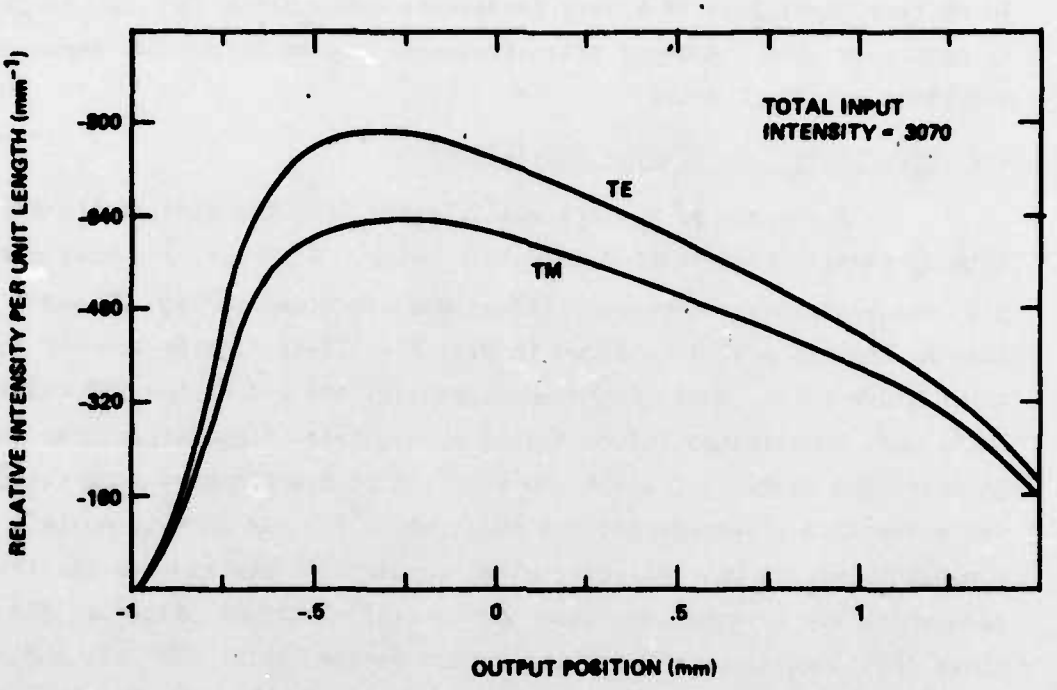

FIG. 21 Light output at end of 3.5 cm $LiTaO_3$ crystal for 85 μm core fiber with NA = .25, three-fold collimation and n = 1.62 AR fluid.

obtained by increasing the index under the spoiler so as to guide the light. This will yield at least another one or two dB improvement, so that 10 dB throughput loss is a very reasonable expectation for this device. As described above, some of this throughput may be traded for improved signal to crosstalk ratio.

4.2 Results for the Spoiler Multiplexer

A variety of spoiler multiplexers were designed, built and tested, as will be described in detail below. A typical 4:1 mask design with the electrode connections illustrated is given in Fig. 22 and a closeup (not to scale) is shown in Fig. 23. These figures are for the top pattern only. Most of the spoiler masks and all of the 3dB coupler masks were complicated enough that they require a computer program to generate the mask. A graphic construction of the computer tape output for a top 12:3 electrode pattern is shown in Fig. 24 (not to scale). Dimensions are in mm. All electrical connections are made to the large pads which are brought away from the central electrode pattern. Fig. 25 shows the computer output for the bottom pattern which has only one electrical connection and is at ground potential. In Fig. 26, sections of the actual mask are shown relative to the entire spoiler design itself. The pattern is too long and narrow to show the entire pattern to scale in one photograph in a reasonable manner.

A total of ten different spoiler multiplexers were constructed and tested with fibers using the same procedure outlined for the 3dB coupler multiplexer and the experimental set up of Fig. 17. Fig. 27 shows the general layout for all the devices and the lettered dimensions on the drawing correspond to the columns of Table 3, which summarizes the characteristics of all ten devices. Photos of SM8 and SM9(12:3) are shown in Figs. 28 through 31.

SM1 and SM2 were the first two devices made and they were designed using the basic procedure illustrated in Fig. 20. SM1 is 2 cm long with two-fold collimation, while SM2 is 3.4 cm long with three-fold

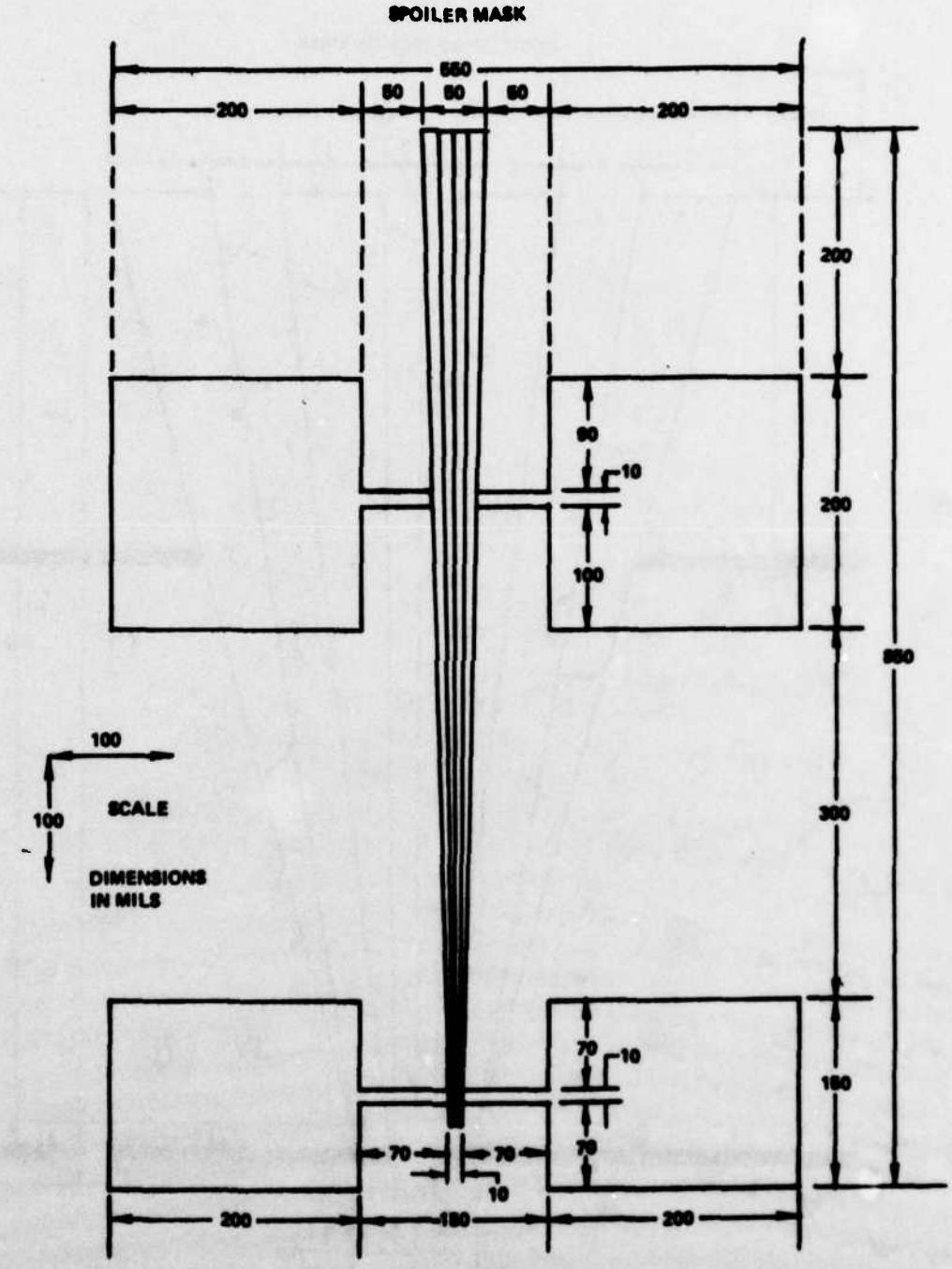

FIG. 22 Mask drawing for top pattern of spoiler mux.

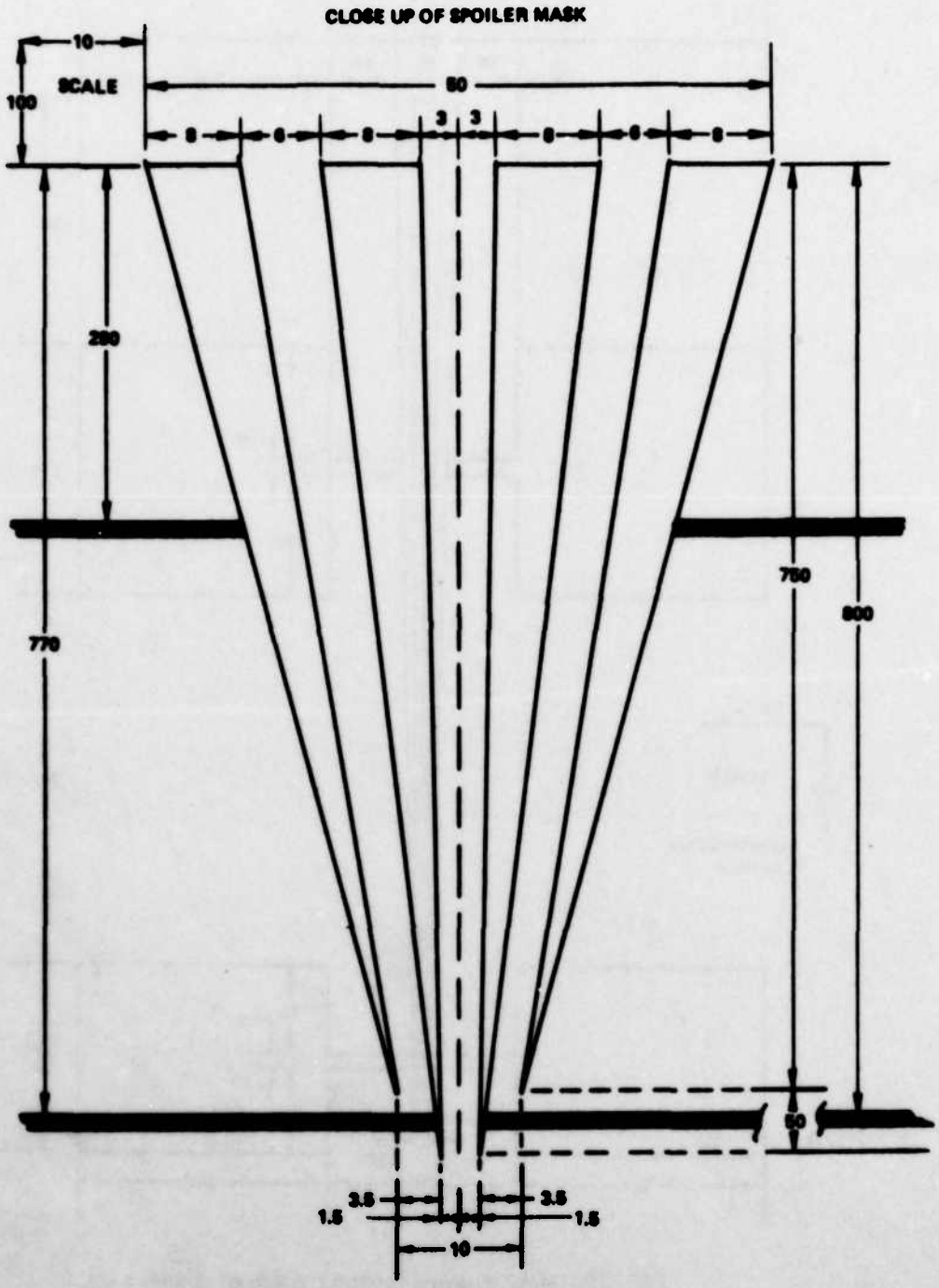

FIG. 23 Closeup of Mask drawing for top pattern of spoiler mux.

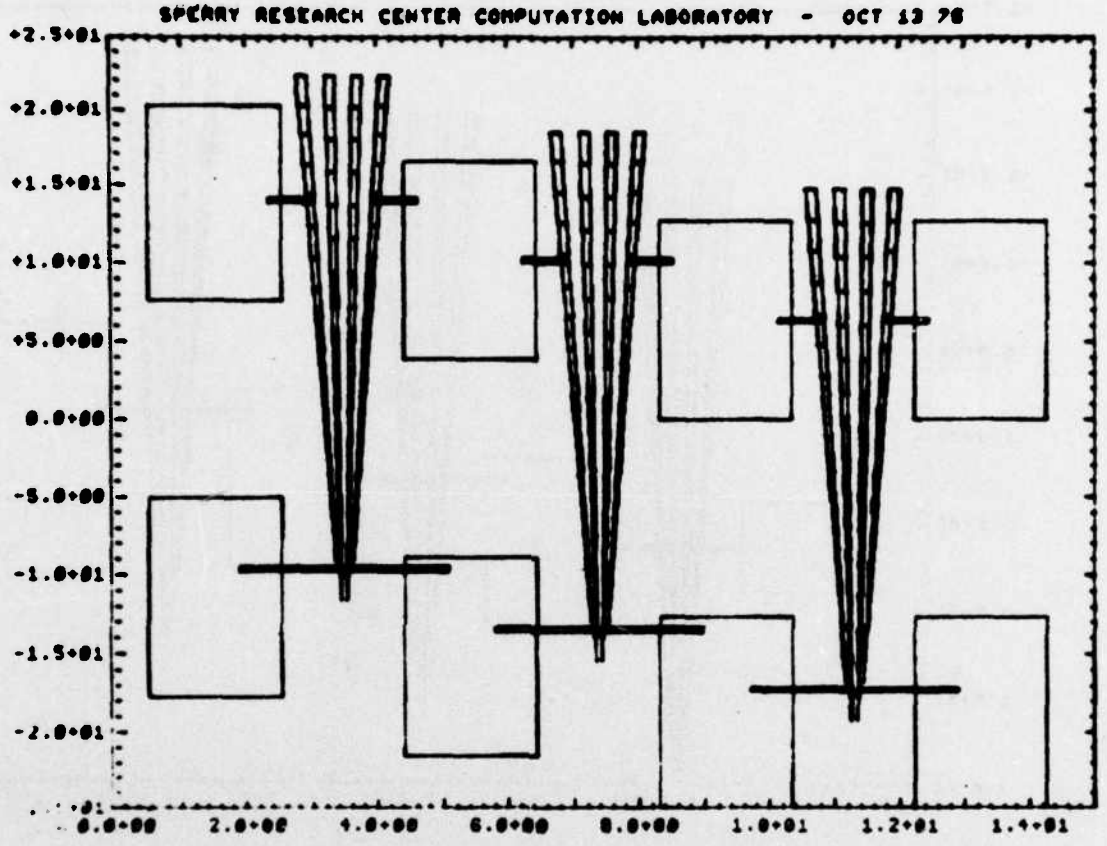

FIG. 24 Computer generated top pattern of 12:3 mux.

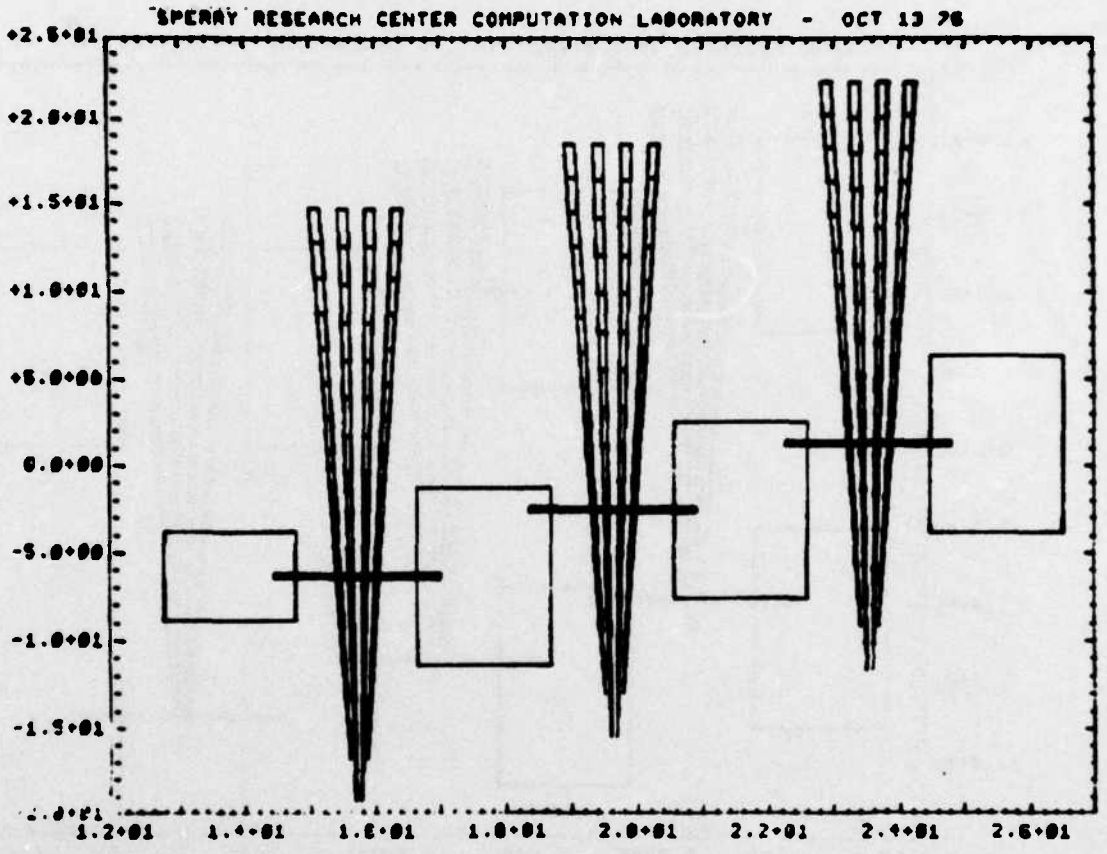

FIG. 25 Computer generated 10 bottom pattern of 12:3 mux.

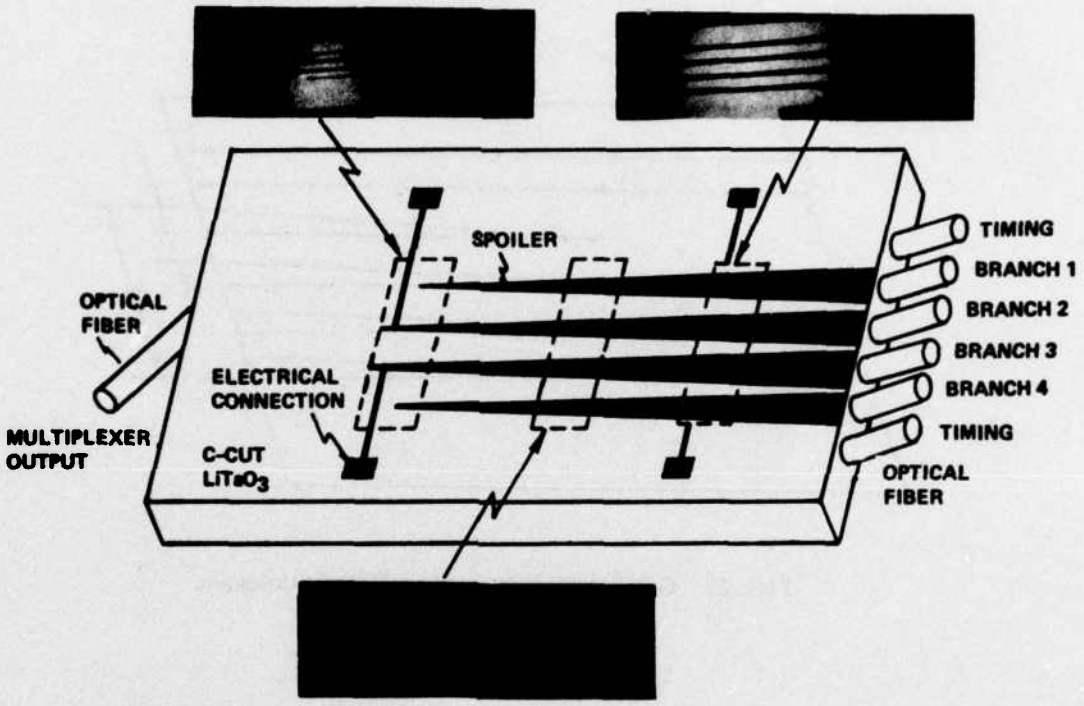

- 15 dB SIGNAL/CROSSTALK
- BANDWIDTH POTENTIAL > 100 MHz
- 12 dB THROUGHPUT LOSS
- 3 cm X 1 cm X 75 μm $LiTaO_3$

FIG. 26 Spoiler mux in use with fibers and illustrated with photos of photoresist mask.

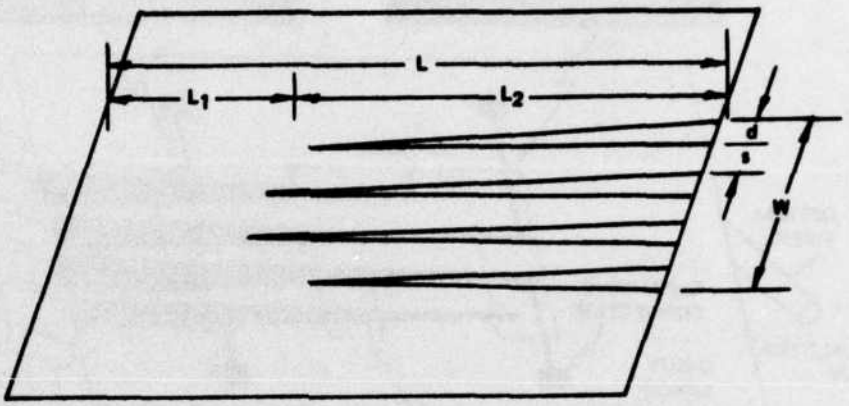

FIG. 27 General pattern of all spoiler multiplexers.

TABLE 3. Spoiler multiplexers constructed under present contract.

DEVICE	L (cm)	L_1 (cm)	L_2 (cm)	W (μm)	d (μm)	s (μm)	Coll.	Loss (db)	S/C (db)	Remarks
SM1	2.0	.5	1.5	1.0	150	125	2	9-13	7-9	S too small
SM2	3.4	1.7	1.7	1.5	250	150	3	10-13	7-8	S too small
SM3	2.1	.3	1.8	1.1	75	275	2	12-20	9-10	L_1 too small
SM4	3.6	1.4	2.2	1.1	75	275	2/1	14-17	12-15	No output coll.
SM5	3.5	.6	2.9	1.4	150	225	2	14-16	9-10	Center electrodes too close
SM6	3.6	1.4	2.2	1.1	75	275	2	11-13	14-16	Final design
SM7	3.5	1.0	2.5	1.1	75	275	2	12-14	14-15	Final design
SM8	3.5	1.0	2.5	1.1	75	275	2	12-14	14-15	Final design (one electrode open)
SM9(12-3)	3.5	1.1	2.4	1.1	75	275	2	12-15	14-16	Final design (one electrode open)
SM10(12-3)	3.5	.8	2.7	1.1	75	275	2	12-15	14-15	Final design

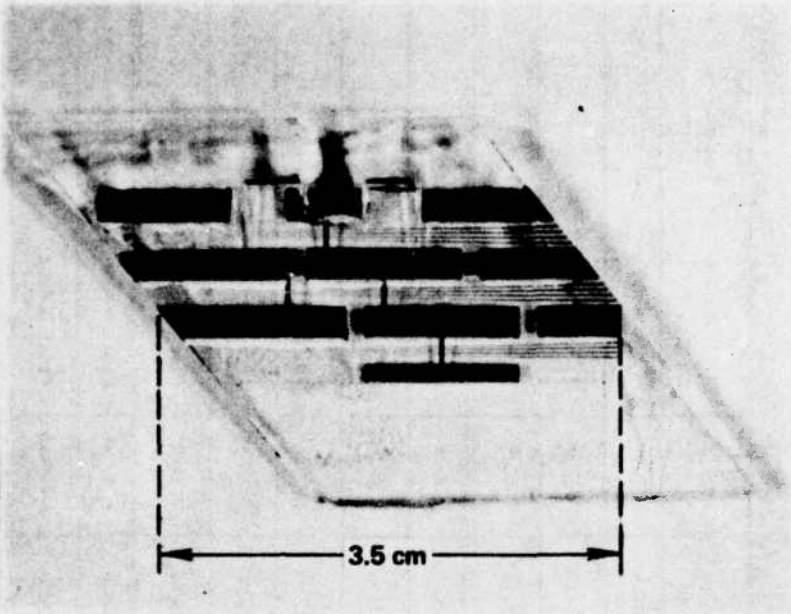

FIG. 28 Spoiler multiplexer SM8 before electrical connectors.

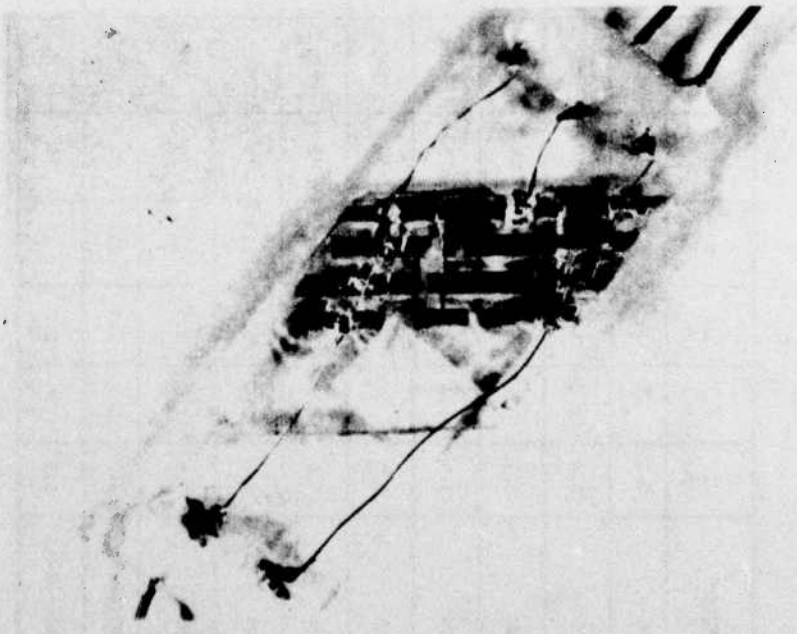

FIG. 29 Spoiler multiplexer SM9 overview.

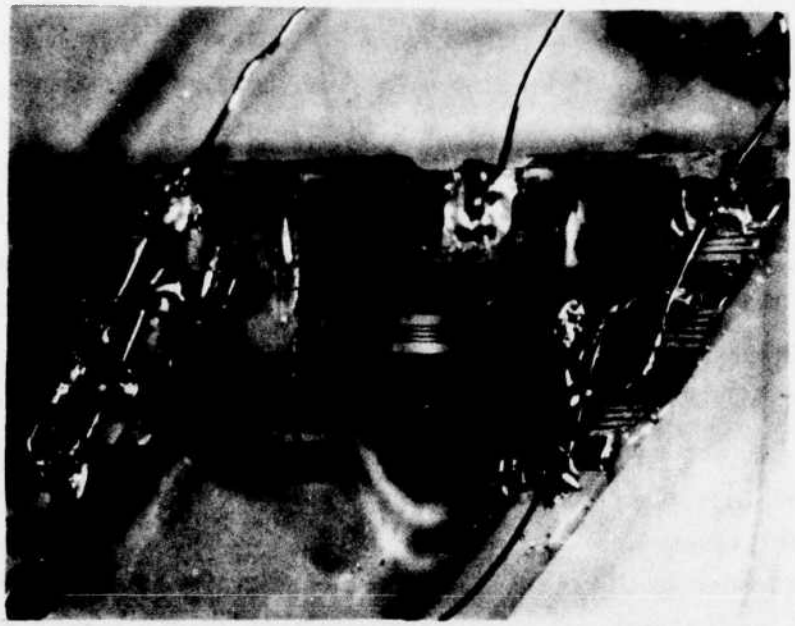

FIG. 30 Spoiler multiplexer SM9, closeup of top.

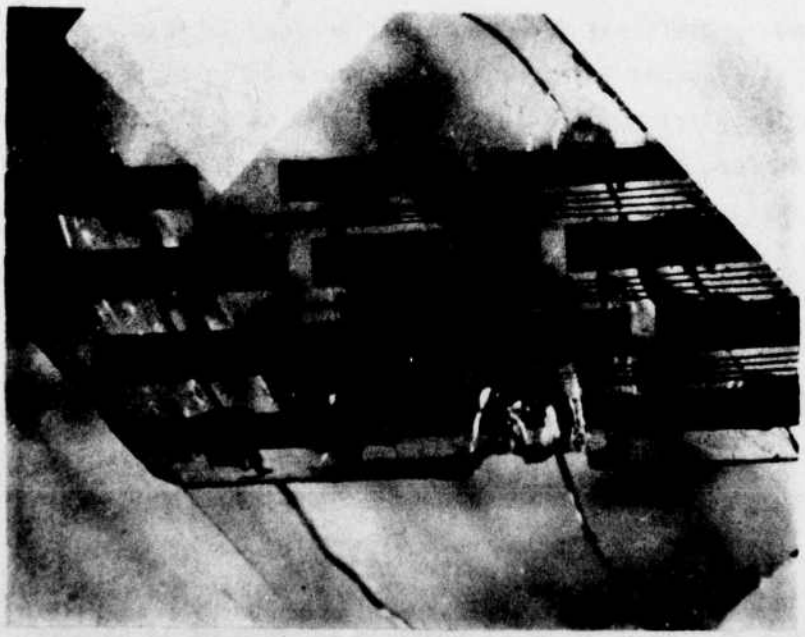

FIG. 31 Spoiler multiplexer SM9, closeup of bottom.

collimation. As explained in Sec. 4.1, the spacing s for this electrode structure is not adequate. The crystal thickness is approximately 75 μm and, at a distance of 75 μm from a pair of opposing electrodes, the electric field (z-component) has declined to only about .2 of its maximum value.[1] For two such pairs of plates the field in the center is about .4 of its maximum value. Thus, the voltage variation has approximately half of its full possible effect. A scan of the output of SM1 is shown in Fig. 32, and the figure indicates a signal to crosstalk ratio of about 7 to 9 dB, similar to that of SM2. This low value is due mainly to the small electrode separation s = 125 μm.

SM3 was constructed next and had s = 275 μm, an electrode separation equal to almost four times the crystal thickness. However, for this device, the electrodes were placed too close to the input fiber, and the light became channeled between the two central triangular electrodes. With the two center electrodes on ("blocking") very little light reached the outer two electrodes, resulting in very high throughput loss for a small improvement in signal to crosstalk.

SM4 is different from the other devices in that no collimation was used on the output in order that the output light could be more easily observed by magnifying and focusing the light on a distant screen. The electrode design, however, was near optimum and 12 to 15 dB signal to crosstalk ratio was achieved. Due to the lack of output collimation the throughput loss was rather high.

For SM5 the electrode spacing was again too small especially at the input end where the electrodes approached to within 75 μm. The signal to crosstalk was low, 9 to 10 dB.

The remaining five devices used the same basic electrode pattern, although the input distance and length were varied. This design used an electrode separation of 275 μm and achieved the maximum signal to crosstalk while sacrificing some throughput power. The devices use two-fold collimation and work well with an NA of about .20. This NA is obtained by

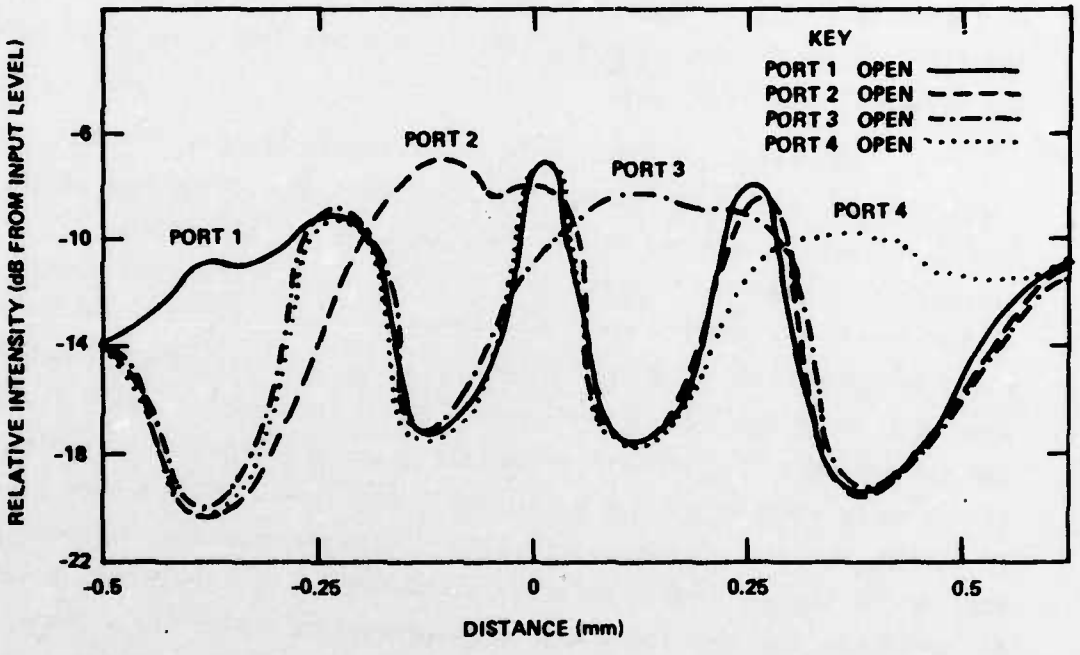

FIG. 32 Performance of spoiler multiplexer SM1

overfilling a Corning fiber with NA = .18. The Corning fiber with NA of .25 and core diameter of 50 μm was felt to be more suitable for the data link than the ITT fiber with NA of .18 and core diameter of 85 μm. More power could be coupled into the Corning fiber, and the core diameter provided a better match with the thickness of the multiplexer crystals. The actual width of the collimated fiber end using two-fold collimation is 170 μm (2 × 85 μm), while the electrode width d was 75 μm. The fringing field increases the effective width of the electrodes so as to "guard" the entire 170 μm fiber port.

SM6 and SM7 exhibited the highest S/C, 14 to 16 dB with ±200V applied to the spoilers. Higher voltages could be used on some of the devices to obtain better S/C. For example, 19dB was the highest S/C obtained, using ±400V on the spoilers, but the multiplexer drivers were designed only for ±200V. Also, the actual increase in S/C is small compared to the penalty paid with the much larger voltage. The throughput loss with +200V applied was less than 15dB in all cases, usually 11-13dB. SM6 and SM7 were the two best 4:1 multiplexers and were packaged with fibers to be used in the 4:1 multiplexed data link. SM8 was very similar in design, but for unknown reasons, one electrode developed an open, and this device was not usable as a 4:1 multiplexer. Figure 28 is a photo of SM8 before the electrodes have been epoxied to the device. Three patterns are visible since the photoresist mask was designed for a 12:3 device, but the crystal size in this case was large enough for only one complete 4:1 multiplexer.

SM9 and SM10 are 12:3 devices fabricated on a single LT crystal. All three 4:1 multiplexers on both devices exhibit approximately the same performance as a single 4:1 device (S/C = 15dB, loss + 13dB) except that one electrode (out of 12) on SM9 is defective. Figures 29 through 31 are photographs of SM9 completed with attached electrodes, but before the fibers have been epoxied to the device. Some portions of the multiplexer are difficult to see due to the layers of glycolphthalate used to protect and bond the crystal.

The capacitance of the spoiler devices was measured at 1 kHz and found to be 15 to 20 pF for one spoiler electrode on a 4:1 device, and 40 to 50 pF for three such electrodes in parallel on a 12:3 device. Thus, the capacitance of the devices will not be a limiting factor in obtaining the required 1.28 MHz bandwidth. However, there is an interelectrode capacitance (7-10 pF) that is about half of the normal capacitance for opposing electrodes, and this interelectrode capacitance increases the complexity of the driving circuitry (see Sec. 6.5).

The device characteristics measured and reported on in this section are ideal in that the device is mounted on a rigid support and precise translation stages are used to accurately position the individual input and output fibers. In particular, the loss and S/C of an output port is recorded for a fiber positioned at the precise optimum position for that port. The theoretical performance of a data link can be extrapolated from such measurements, but a much more severe test occurs when fibers are rigidly attached to the device and the entire unit is packaged as a unit. This procedure is described in the next section.

5. FIBER/DEVICE COUPLING AND PACKAGING

5.1 Fiber/Device Connections

One of the more important tasks to be completed in fabricating a fiber optic switch is the permanent and secure connection of the optical fiber to the device. The fiber connections required for a 12:3 spoiler multiplexer (or demultiplexer) are shown, without non-normal incidence butt coupling, in Fig. 33. Of course, a 4:1 multiplexer requires only one-third of the input and output fibers shown in the drawing. Each 4:1 multiplexer uses four signal information carrying fibers for input with each fiber positioned exactly in front of one electrode. In addition, two fibers are included on either end of the four-spoiler array for carrying the timing and synch pulses. These outer two fibers have somewhat lower throughput than the central four fibers, but the two fiber redundancy is generally sufficient for an adequate signal. Also, shown in Fig. 33 are the correct

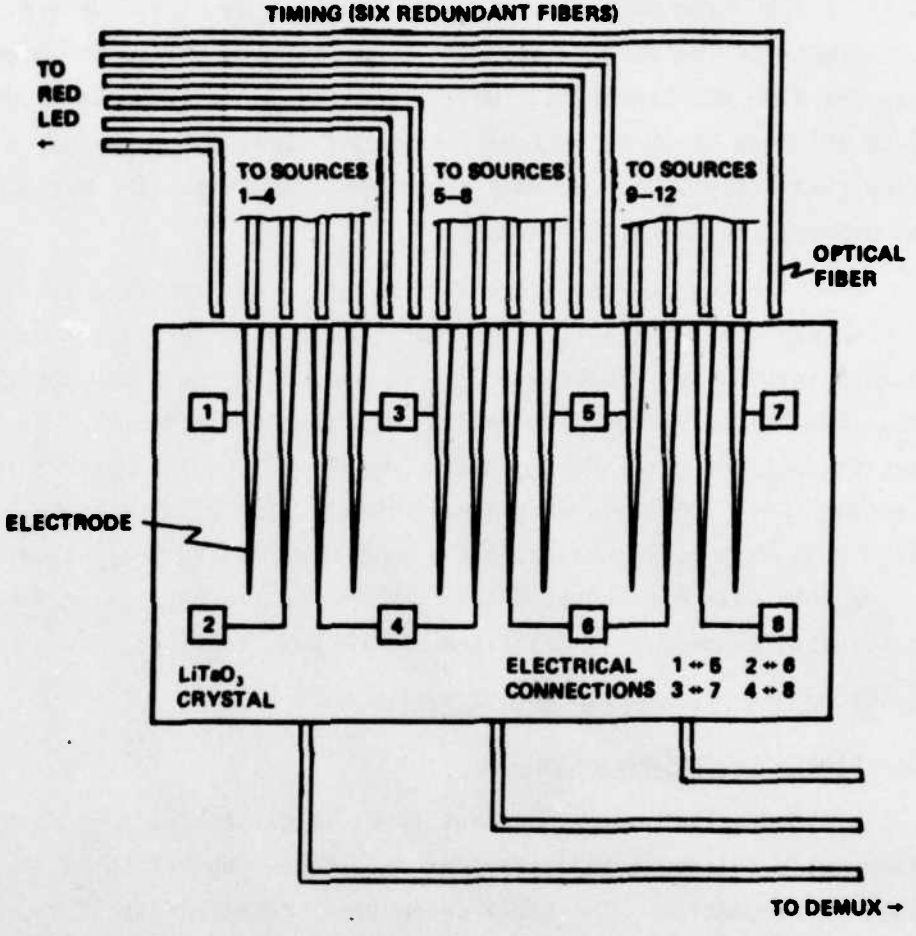

FIG. 33 Optical and electrical connections for the 12:3 multiplexer.

electrical connections for parallel operation of a 12:3 device with pad 1 connected to pad 5, pad 2 to pad 6, etc.

5.2 Fiber Terminations

The final design for the spoiler electrode multiplexer uses electrodes spaced on 400 μm centers. Used with 2:1 collimation, this requires that an array of fibers be formed accurately spaced on 200 μm centers, while the Corning fiber chosen for the link has 125 μm cladding diameter. A series of accurate grooves are required to correctly align and hold the fibers before epoxying in place and polishing. It was felt that only a photolithographic process would have the required accuracy in defining such a pattern, and a mask was designed consisting of a series of three sets of six lines spaced on 200 μm centers and varying in width from 25 to 175 μm. Several methods were considered for actually forming the grooves themselves: etching glass with HF, preferential etching in silicon, or exposing a thick photopolymer such as Riston.[8] The first two methods were used successfully, while time limitations prevented an adequate test of the Riston.

The glass etching procedure is the simplest, although it does not produce the best grooves. A glass slide is cleaned and then baked at 150°C, and then evaporated with a flash of Cr and 3000Å of Au. The slide is coated with resist, exposed, developed and baked at 150°C for an hour. The Cr and Au are then removed from the grooves with commercial etchants. The glass slide is placed in a HF solution and ultrasonic for 100 to 200 sec. Figure 34 shows an end on view of one such glass slide. The best grooves are straight, round and quite smooth, but usually a depth of only about 50 to 70 μm can be obtained. However, this is enough to hold the fiber temporarily for epoxying.

Preferential etching in silicon[9] has been used for several years in integrated electronic circuit technology and more recently[10] in fiber optics for aligning fibers. A 3000Å layer of SiO_2, grown on

FIG. 34 Photograph of optical fiber alignment grooves made by etching glass. Groove width at top of glass is 125 μm.

a .5 mm thick (100) wafer of Si, is used as the mask for the etching of Si. The pattern is etched in the SiO_2 first with standard photoresist techniques and buffered HF. Then a KOH-alcohol system[9] is used to etch the Si grooves defined by the SiO_2 layer. The etching is highly preferential in that the etch rate for the ⟨100⟩ direction is about 50 times that of the ⟨111⟩ direction. If the grooves are placed in the ⟨110⟩ direction on the (100) wafer, the result is a triangular shaped groove with smooth sides. The width is almost entirely fixed by the width of the initial mask opening. Figure 35 is a photograph of a Si substrate etched about 75 μm using this technique. With further etching, the bottom of the groove descends deeper until a triangular groove is formed.

The grooved glass or silicon wafer is next epoxied to an aluminum base. The individual fibers are placed in a PVC jacket, and this bundle is clamped in place on the aluminum base. The plastic protective coating is removed from about 2 cm of the ends of the fibers, and the fibers are laid in the grooves and epoxied in place. The assembly is then cut on a diamond saw at the correct angle and the ends of the fibers are polished. A completed unit is shown in Fig. 36. The technique for holding the fibers in the grooves while epoxying is not satisfactory and results in error in the positioning of the fibers (i.e., they are not perfectly uniformly spaced as can be seen from the photograph). This misalignment does contribute to a reduction in signal to crosstalk ratio (perhaps, 2 to 4 dB) and is therefore important. However, it is felt that, with more care, future fiber holders can be made more precise.

5.3 Packaging

After the fiber connectors have been fabricated, they are epoxied to the device. The procedure is as follows: first, with the device mounted on an optical post, the input fiber connector is temporarily fastened to a precision translation device. The optical output from the device is monitored as the input fiber is adjusted for the exact correct position, and then the connector and device are epoxied.

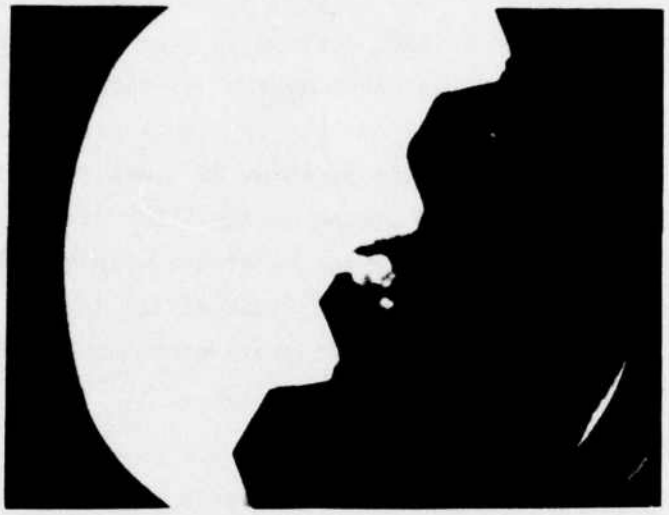

FIG. 35 Photograph of optical fiber alignment grooves made by preferential etching in silicon.

FIG. 36 Photograph of a completed optical fiber termination cut and polished at 23°.

The procedure is repeated with the output connector. An index fluid[1] (n = 1.6 to 1.7) is used between the fibers and device to reduce reflection losses. This fluid is relatively non-volative and should last at least several months, although the exact length of time is not certain. The fluid is easily replaced if it does eventually evaporate. Future fabrication improvements would include sealing the interface so that the index fluid is permanently in place or using a high index, clear cement.

It was anticipated that, in epoxying the multi-fiber connectors to the device, the performance would deteriorate over the ideal lab test measurements. Before epoxying, the devices had an inherent, with optimum fiber placement, 14 to 16 dB signal to crosstalk ratio. Afterward, the performance had decreased to 10 to 13 dB. There are two reasons for this degradation: the fibers were not perfectly positioned as mentioned above and the connector units were not perfectly aligned or shifted slightly during the epoxying. The throughput loss is generally unaffected, but the S/C ratio is much more sensitive to positioning, since this ratio is a strong function of the leakage of light contributing to crosstalk, which is inherently a very small quantity. Therefore, this ratio is very intolerant to small deviations of the fiber from the ideal position. However, it is felt that future improved fabrication procedures should reduce the approximately 4 dB degradation of S/C. suffered by these first attempts at fiber/device packaging.

Another problem was encountered in attempting to epoxy the eighteen-fiber input connector and 3-fiber output connector to the 12:3 multiplexer. In this case, the positioning problem is much more severe, since tolerances of about 50 μm must now be maintained over distances of 5 mm, the distance between 4:1 multiplexer patterns. With the 4:1 devices the same absolute accuracy of 50 μm was required, but only over distances of .5 mm (an order of magnitude reduction). The problem is made severe by the 23° termination angle that is used for coupling. An error in that angle will cause a positional error in the fibers when they are joined to to the device. A positional error of less than 50 μm over the 5 mm

distance between 4:1 multiplexers requires an angular accuracy of less than .16°. The fabrication procedures used for making the angular fiber terminations and sawing the crystals relative to the multiplexer electrode pattern are not within the required accuracy. This precluded the development of a complete packaged 12:3 device. It is felt that if it is necessary to have several devices on a single crystal then the procedures could be refined to obtain the desired accuracy in the future. At present, however, procedures are only available for a single multiplexer on a crystal when angular butt coupling collimation is used.

A set of two completely packaged 4:1 multiplexer/demultiplexers are shown in Fig. 37. The electrical connector pins mate directly with the multiplexer driver. The fibers are contained in the PVC jackets and are ready for mating with the source, detector, or fiber/fiber connectors.

6. DATA LINK COMPONENTS

6.1 Optical Fiber

The design of the multiplexer depends to some extent on the characteristics of the fiber chosen, mainly core diameter and NA. As previously described, the present optimized spoiler multiplexer was designed based on a fiber with a core diameter of about 85 μm and NA = .20. However, the same devide without modification will still give quite reasonable performance using a range of core diameters from 50 μm to 100 μm and a range of fiber NA from .15 to .25. Over these ranges, the signal to crosstalk ratio of the device will actually remain unchanged, and only the throughput loss will be affected. For smaller core fibers the output coupling loss will increase, while larger core fibers increase the input coupling loss. A fiber with larger NA causes light to spread beyond the array of output fibers, and a fiber with a smaller NA results in less light impinging on the outer fibers of the array. However, the throughput loss should not increase by more than about 2 dB over the ranges listed above.

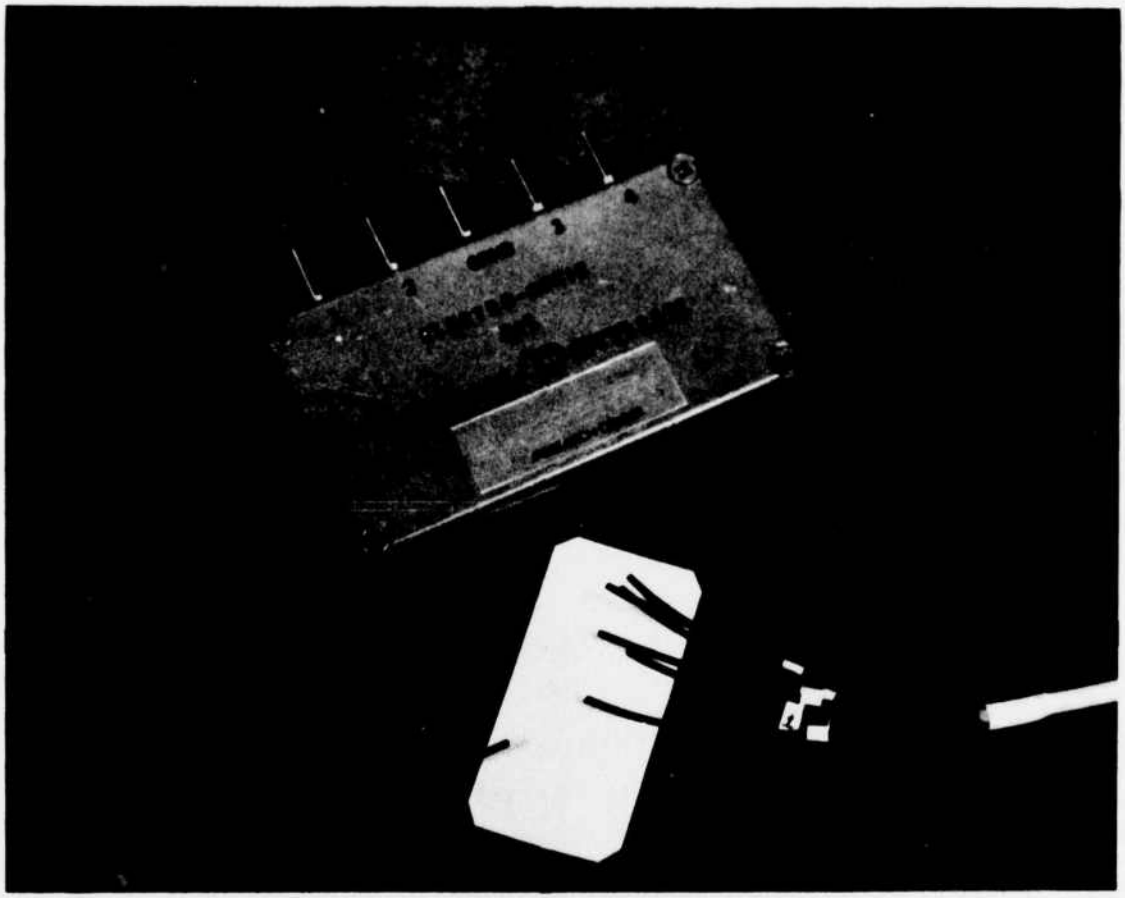

FIG. 37 Packaged multiplexer (or demultiplexer) unit with input and output fibers. Unit measures 11 X 6 X 3 cm.

Some of the commercially available fibers at present have specifications that fall outside the ranges given above for the final spoiler multiplexer. Restricting consideration to low loss, (<20dB/km), multimode fibers, the core size may range from 50 μm to about 250 μm and the NA may be from .14 to .30, and perhaps .40 for some fibers with plastic claddings. The all glass fibers (glass core and glass cladding) generally fall within the range that is useful with the present spoiler multiplexer. Some of the plastic clad fibers have been made with larger core diameter and larger NA in order to capture more optical power from LED sources. The increased NA can be handled quite well with the basic spoiler multiplexer arrangement, if the present design incorporates some modifications that are easy to implement, mainly constructing the crystals and fibers for three-fold collimation instead of two-fold collimation. Experiments have been done with three-fold collimation devices that show such a procedure is no more difficult to use than two-fold collimation; however, an extra 1 dB total reflection loss per device was observed for this larger incident angle.

The large-core-diameter fibers can be used if the thickness of the crystal is made larger so as to limit coupling losses to acceptable values. For example, the 125 μm diameter core should use a crystal thicknexx of 80 μm or more and the 250 μm diameter fiber would require approximately a 160 μm thick crystal. This latter thickness using the present electrode design would require approximately twice the voltage to achieve the same signal to crosstalk performance, and this could be a problem when the required multiplexer driving rate is more than 1 or 2 MHz.

The actual fiber epoxied to the devices and used for the multiplexed optical data link is made by Corning and has 85 μm core with .18 NA, which for short distances can be increased to .20 NA. The fiber was chosen over the other primary candidate, an ITT fiber with 50 μm core and .25 NA,

because more power is coupled into the larger core Corning fiber when using most LED sources. Estimating the power coupled as proportional to $(NA)^2 \times (\text{core dian})^2$, the Corning fiber has a better performance by a ratio of 1.85:1.

6.2 Source Considerations

The best source for use with the multiplexed optical data link is a Burrus-type, GaAlAs LED. Only the Burrus geometry, where the fiber is integrally butt coupled to the active emitting area, can couple reasonable amounts of power into a single, small core glass fiber. The GaAlAs composition is preferred because it can be made to emit in the .82 to .85 μm wavelength range which is the low loss region for most fibers, as opposed to the GaAs maximum wavelength of .9 μm where the loss is higher. The LED is preferred over a laser due to its higher reliability, better lifetime, and much easier drive requirements. It is only recently that semiconductor laser sources have become available that will operate cw or 50% duty cyle at room temperature, and the commercially available devices are still somewhat unreliable at this time.

Unfortunately, the Burrus-style LED is not readily available commercially at a reasonable cost. Bell-Northern and Plessey have developed this type of LED, and coupling of .5 to more than 1 mW of optical power into a single glass fiber appears possible. However, at this time the cost of these devices is high. Except for very elaborate coupling schemes that involve lenses or other means for focusing light, most large area LEDs will not couple a reasonable amount of power into a single glass fiber. About 50 μW of power coupled into the input fibers is required for a fair demonstration of the multiplexed optical data link. Most of the non-Burrus LEDs that were tried could not achieve this power but rather were limited to less than 10 μW input power. One exception to this is a very high power (40 mW) LED from Hitachi (HLD-20) that coupled in 50 μW. However, this coupling was achieved by placing the fiber extremely close to, although not touching, the active area of the diode. This is a very high

risk procedure since touching or contaminating this surface will eventually destroy the performance of the LED, and these devices are also fairly costly.

Not having any reasonable LED to use as an alternative, a cw laser from Laser Diode (LCW-5) has been chosen to demonstrate the data link. This is not a very satisfactory choice mainly for the reasons mentioned above; that is, these diodes seem to be quite unreliable at this time. The maximum operating temperature is specified as 27^{o} C, and extensive heat sinking is required. A thermoelectric cooler was used with the diode for this purpose. The device is capable of coupling 50 μW into a single fiber with the window on. With the window removed and the fiber butted very close to the active surface, more than one mW can be coupled into a fiber, but operating in this manner eventually leads to contamination of the surface and degradation of the diode's performance.

The semiconductor laser (LCW-5) supplied with the optical data link is driven by a circuit that provides the required 200-250 mA drive current and produces a 32KHz square wave. The unit is self-contained except for .5 amp at -10Vdc that must be supplied to run the laser externally and 1 to 5 amps that is required for the thermoelectric cooler.

6.3 Detector and Preamp

The bandwidth required to demonstrate and thoroughly test the performance of the multiplexed optical link is approximately an order of magnitude greater than the bandwidth actually needed in normal operation when the receiver is used only to recover the original 32 kb/s data. For testing and demonstration purposes one wishes to resolve and measure the individual optical pulses provided by the multiplexer, and these pulses occur at a 320k H_z rate with a rise or fall time of 100 nsec. Thus, the bandwidth required for test purposes is several MH_z, while for actual operation of the data link several hundred kH_z is adequate.

The detector used for the measurements of Sec. 7 is an EGG,

Type SHS-100, PIN photodiode, with a $5mm^2$ active area and a capacitance of 4 pF. The diode chosen is moderately priced and was selected over an avalanche photodiode for the sake of simplicity and cost.

For the test measurements of Sec. 7, straight detection (photodetector plus resistor) was used for simplicity whenever the received optical signal strength was adequate. This was generally the case when the multiplexer device was tested and the throughput losses were low. However, since less than 50 μW was generally coupled into the optical fiber, amplification was a necessity when the full data link was used. The schematic of the preamp circuit used for these measurements is shown in Fig. 38.

6.4 Fiber Connectors

The data link requires fiber connections at several points other than for the multiplexer and demultiplexer input and output. These connection points are source-to-fiber, fiber-to-detector and fiber-to-fiber, for joining the output of the multiplexer with the input of the demultiplexer. Permanent splices and connections were not used in order to maintain the integrity of the individual multiplexer and demultiplexer units and to allow for further experimentation.

The fiber-to-fiber coupler is shown in Fig. 39. Basically, it consists of a grooved plexiglass substrate and two top pieces of plexiglass that are held with screws and clamp the input and output fibers in place. Overall dimensions are 4.4 cm × .6 cm × .6 cm. The connection procedure does take care, but will yield nonpermanent connections of less than one dB loss for small core diameter multimode fibers.

The fiber connections for the source and detector operate in a similar manner. A grooved piece of plexiglass has been permanently attached to the source and detector units so that a fiber lying in the groove matches well with the particular device. The fiber PVC jacket is held in place by a plastic clamp piece, and the fiber is maneuvered into

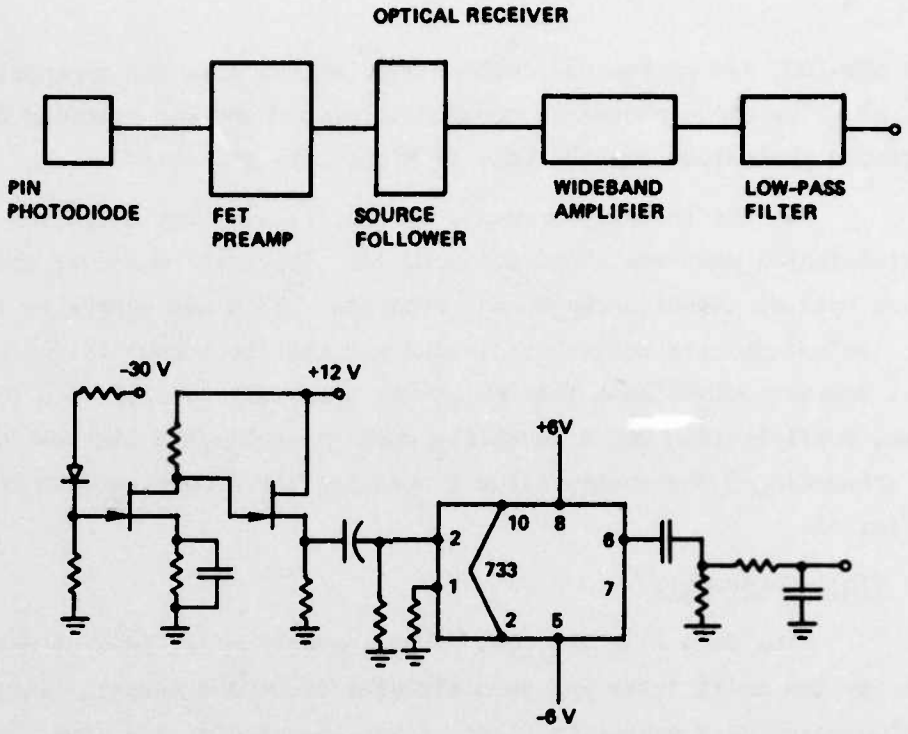

FIG. 38 Circuit diagram of optical receiver.

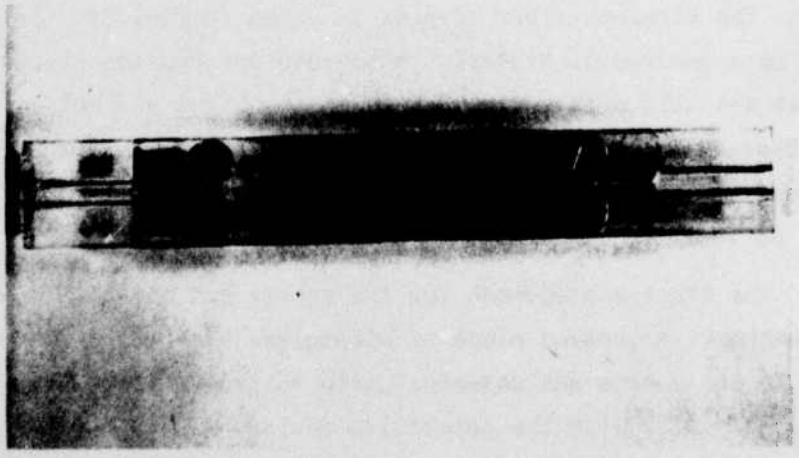

FIG. 39 Fiber-to-fiber connector.

the groove and held there with fluid or tape. Since the fibers are held away from the active source or detector area by a window, the exact transverse positioning is not extremely critical. However, the input coupling does suffer because of this distance between the source and fiber, and less than 50 μW of power is coupled into the fiber from a 5mW laser source. The fiber to detector coupling is much less critical, and the output coupling losses are low.

6.5 Multiplexer Driver Electronics and Synchronization

The multiplexer or demultiplexer driver is housed in a 14 x 25 x 15 cm enclosure as shown in Fig. 40 and is equipped to allow the packaged multiplexer to plug directly into the side of the driver unit. A block diagram of the electrical circuit for one of the four driver channels is shown in Fig. 41. Each driver unit consumes less than 50W of power and is air cooled by a fan mounted inside of the cabinet.

The electrical output for each of the four channels is shown in Fig. 42. The pulse repetition rate for each individual channel is 320KH$_z$ as required to sample a 32Kbit/s input signal ten times per pulse. The actual rise or fall time of each pulse is about 100 nsec. The voltage range of the signal is fixed by two external supplies that must be provided separately. These supplies fix the base voltage and voltage peak and are arbitrary in magnitude except that the difference in voltage between the two supplies should not exceed the 400V that is normally used with the spoiler devices. For example, most of the measurements in the next section were taken with the driver base line at -200V while pulsing to +200V or at -350V pulsing to +50V. The two external high voltage dc supplies must be capable of delivering about 100 ma apiece. In addition, two 5V supplies are required that will provide approximately 1 amp each. If proper electrical connections are made, one driver can easily drive both the 4:1 multiplexer and demultiplexer or a 12:3 multiplexer without any significant added power consumption over that required for a single 4:1 device.

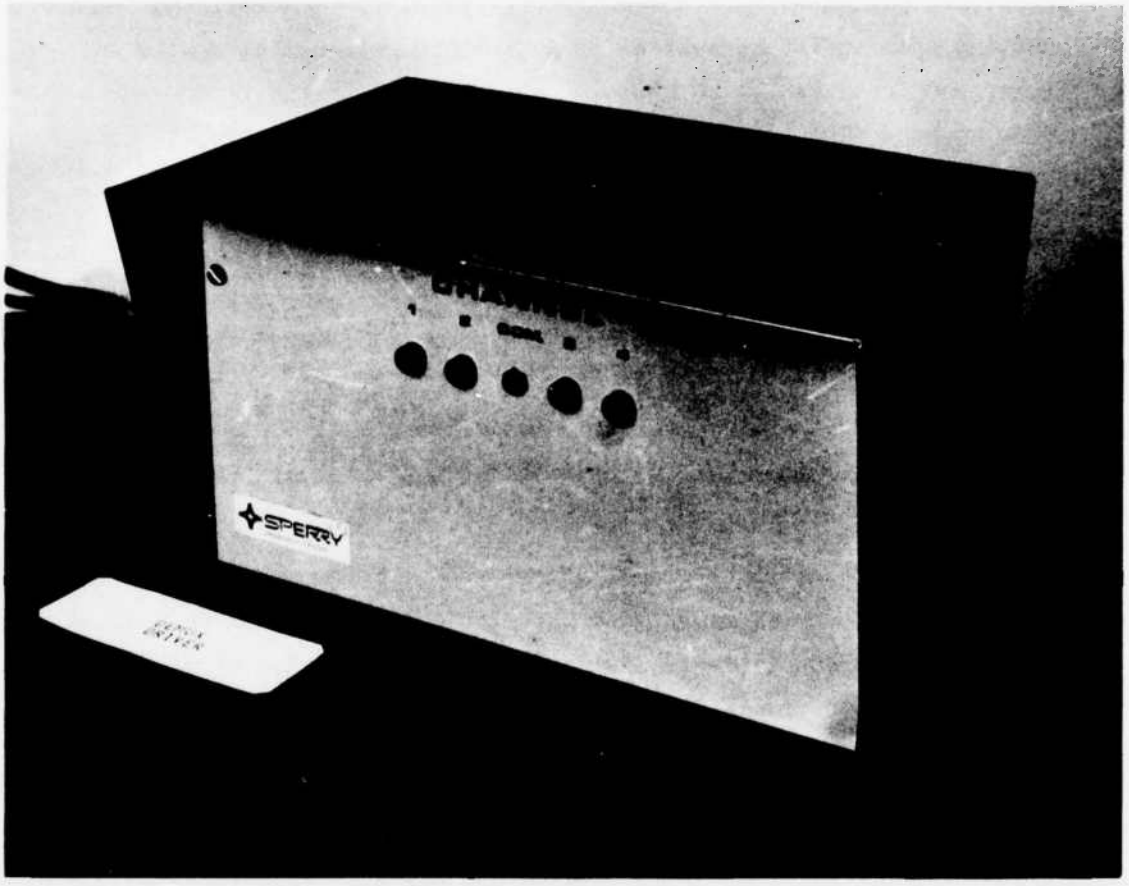

FIG. 40 Multiplexer driver. Unit measures 14 X 25 X 15 cm and consumes less than 50 W.

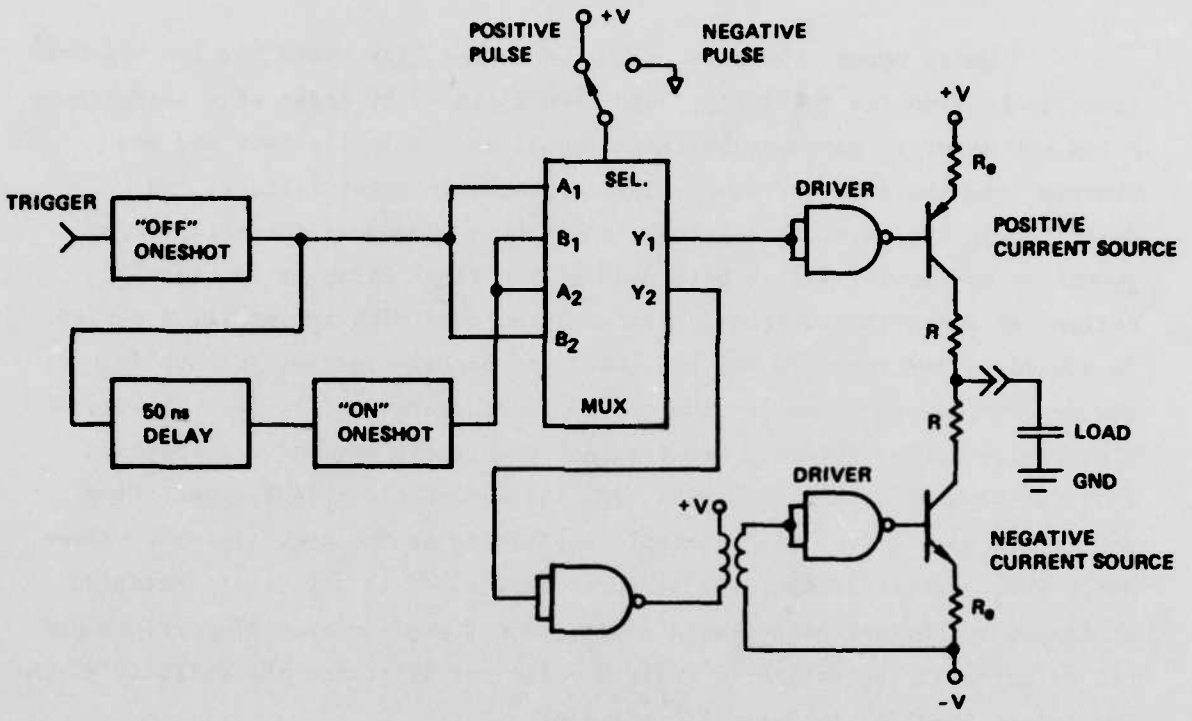

FIG. 41 Circuit diagram of multiplexer driver.

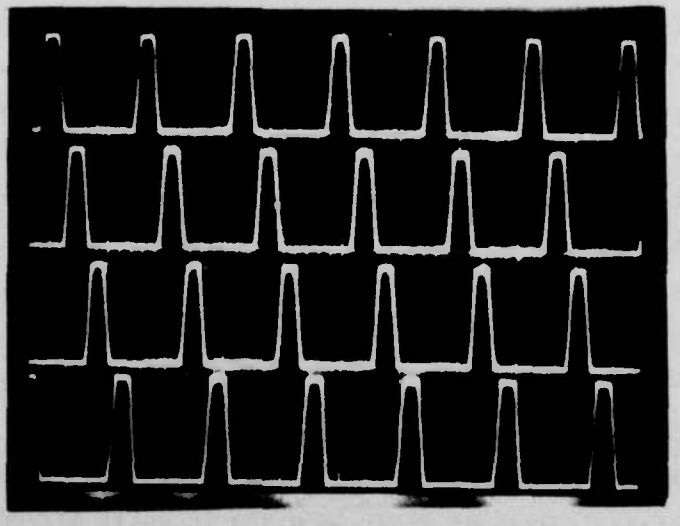

FIG. 42 Output voltage from four channels of multiplexer driver.

Under normal operating conditions, the link would provide synchronization between the multiplexer and demultiplexer by means of a signal from a red LED added to the main infrared signal at the multiplexer end and removed from the demultiplexer end by appropriate color filters. As described in the previous sections, the fibers necessary for this timing operation are positioned at both ends of the fiber array in the spoiler design and these timing fibers have been included with the packaged device. In addition, two separate drivers have been constructed for the multiplexer and demultiplexer so that timing can be incorporated easily into the driver electronics in the future. However, optical timing was not incorporated into the present multiplexed link, and instead an electrical signal from the multiplexer driver also controls the timing on the demultiplexer driver. While this electrical approach is much simpler, it is felt that inclusion of timing by optical pulses should not present any fundamental problems and can be added in the future if desired while not affecting the validity of the experiments made on the present test link.

7. MULTIPLEXED OPTICAL DATA LINK

7.1 Single Multiplexer Unit Performance

The performance of the two individual multiplexer (or demultiplexer) units shown in Fig. 37 were first tested individually using the experimental arrangement of Fig. 43. The GaAlAs laser source was coupled to the input fiber of one of the devices used as a demultiplexer, while a PIN photodiode monitored each output fiber individually. (The performance of the device when used as a multiplexer is identical.) Both dc voltages and the high-frequency multiplexer driver were used in the experiments. The link was also qualitatively tested with a Plessey LED source and similar results were obtained.

The results of the dc tests are given in Table 4 for the unit labeled MUX 2. The results for MUX 1 are similar. In the table the power level out of an individual fiber is given in units of -dB down from the input level and as a function of a given voltage applied to the electrode

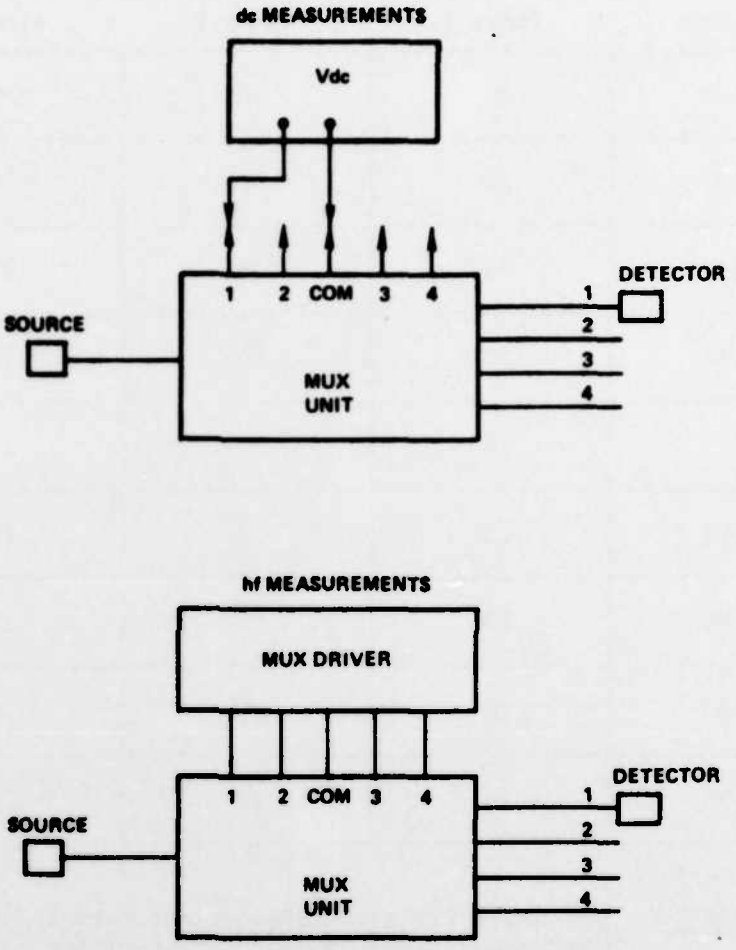

FIG. 43 Experimental arrangements used for dc and high frequency measurements of an individual multiplexer or demultiplexer.

Voltage	Fiber 1	Fiber 2	Fiber 3	Fiber 4
-400	32	30	>29	>31
-300	30	28	>29	>31
-200	26	25	29	31
-100	20	21	22	23
0	17	17	15	16
100	15	16	13	15
200	16	15	13	15
300	16	15	13	15
400	16	14	13	15

TABLE 4. Throughput for each fiber output port in dB down from the input power level, as a function of the voltage applied to that port for multiplexer 2.

that corresponds to that fiber. From the table the throughput loss and signal to crosstalk ratio can be found for any operating voltage levels. For a maximum voltage swing of 400 V, the optimum operating points appear to be about -200 V to +260 V. For this range, the throughput is about 15 dB down, and the signal to crosstalk ratio is 13 to 16 dB.

The signal to crosstalk ratios for an individual multiplexer unit using the high frequency driver are given in Table 5 for two different voltage ranges: -350 to +50 and -200 to +200 volts. The -350 to +50 volt range yields far superior performance, 11 to 14 dB signal to crosstalk ratio, as opposed to the -200 to +200 volt range, 4 to 7 dB. This trend could be predicted by the dc measurements of Table 4, but the crosstalk is, in general, higher for the high frequency case than for the dc measurements. In particular, it is harder to turn an output port "off"; that is, a stronger negative pulse is needed to reduce the output than would be predicted from the dc measurements. The exact cause of this behavior is not known at this time.

Oscilloscope traces for each output port are shown in Fig. 44 for the -350 V to +50 V range and in Fig. 45 for the -200 V to +200 V range. The optical signal supplied by the source is a 32 kHz square wave while the demultiplexer samples the signal ten times per cycle as shown. The signal to crosstalk ratio can be read directly from the photos as the ratio of the peak signal height to the signal strength in the valley between the peaks.

In order to illustrate the relative timing of the optical signals, two detectors were used in the experimental setup of Fig. 32, and the output response is shown in Fig. 46. Figure 46(a) is for channels 2 and 3, Fig. 46(b) for channels 3 and 4, and Fig. 46(c) shows channels 2 and 4, all using -350 to 50 V.

7.2 Complete Multiplexed Link

For the final testing both units were assembled in the simulated multiplexed optical data link shown in Figs. 47 and 48. Due to cost considerations only one source was available for the input of the 4:1

CHANNEL	(S/C (+50/-350)	S/C (+200/-200)
1	12 dB	5 dB
2	11 dB	4 dB
3	13 dB	6 dB
4	14 dB	7 dB

TABLE 5. Signal to crosstalk ratio of Multiplexer 2 using the high frequency driver.

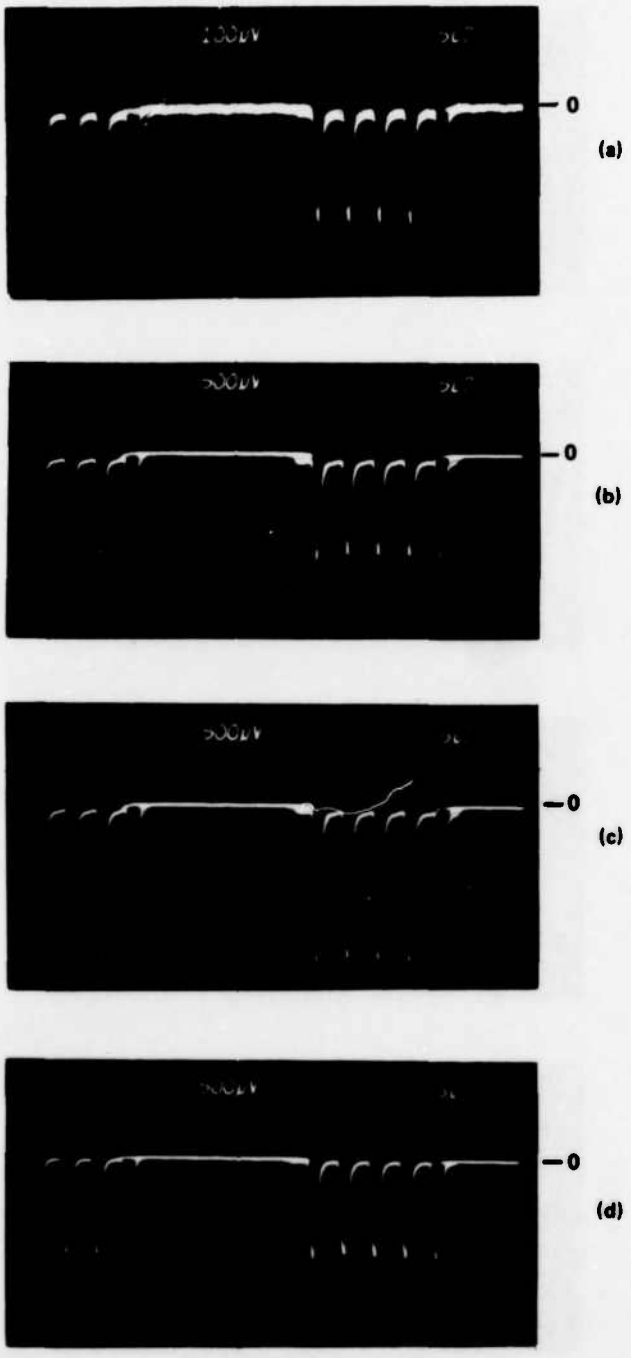

FIG. 44 (a) – (d) Output from channels 1 through 4 using the experimental arrangement of Fig. 43 and the high frequency multiplexer driver switched between -350 V and +50 V. Pulses are negative.

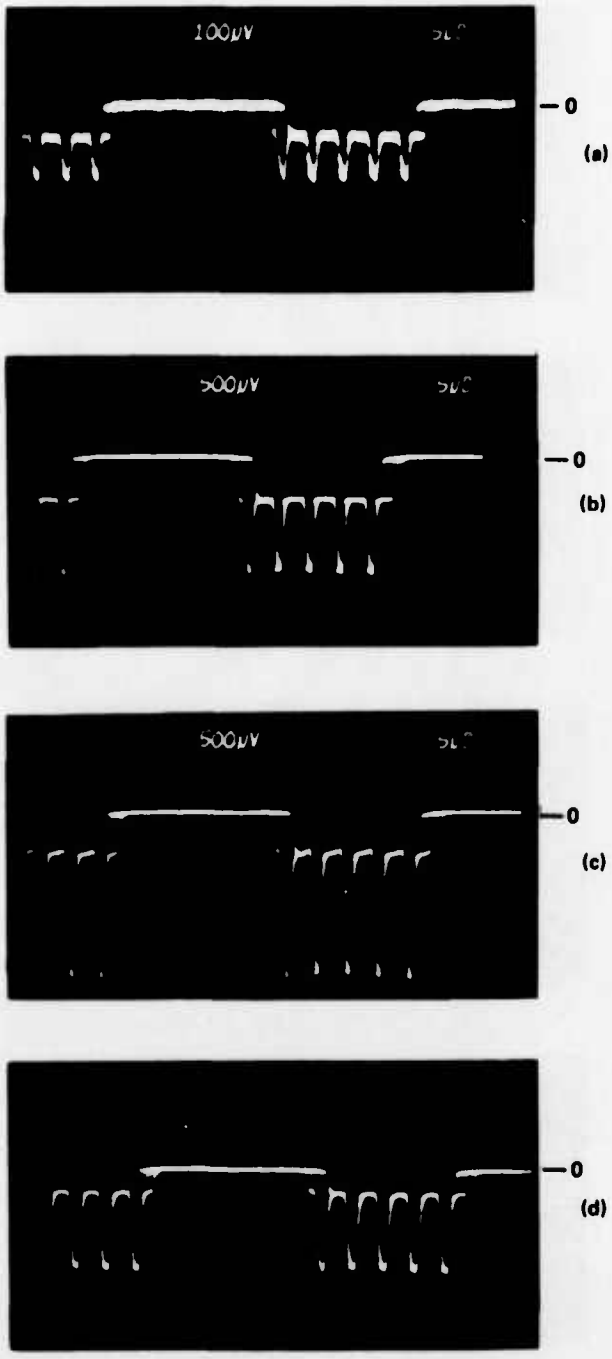

FIG. 45 (a) – (d) Same as Fig. 44 with V = -200 and +200 Volts. Pulses are negative.

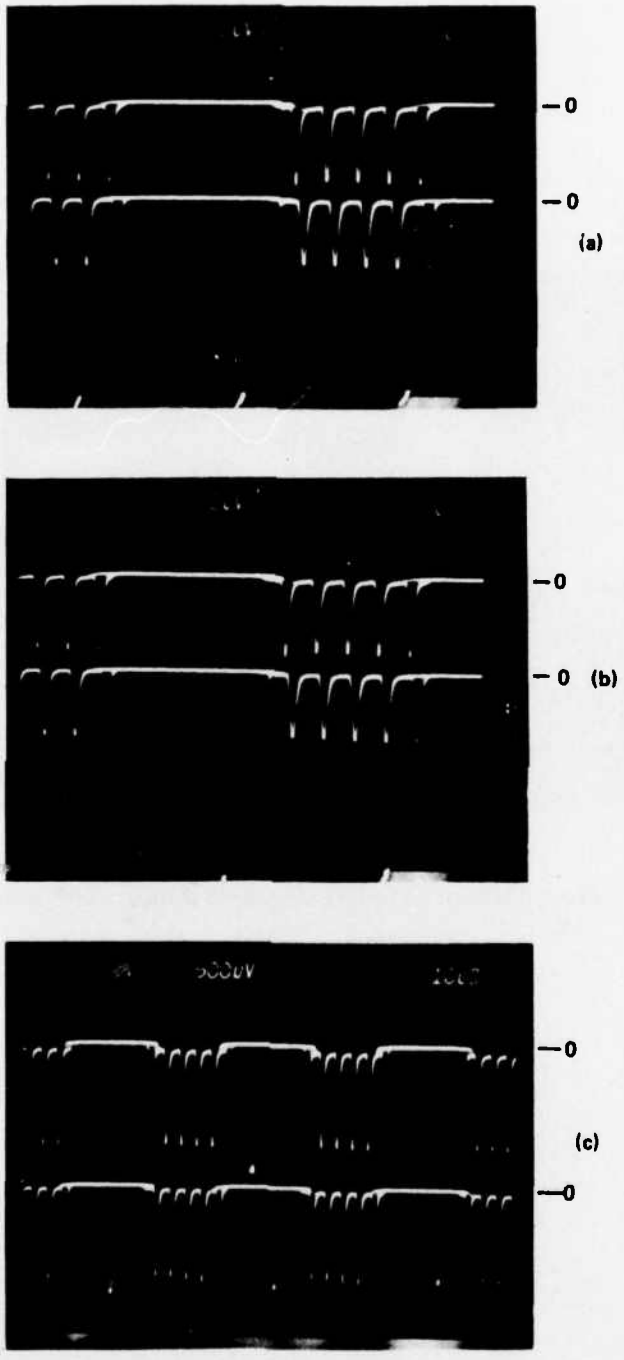

FIG. 46 (a) – (c) Two output channels from a demultiplexer unit. (a) Channels 2 and 3. (b) Channels 3 and 4. (c) Channels 2 and 4. Pulses are negative.

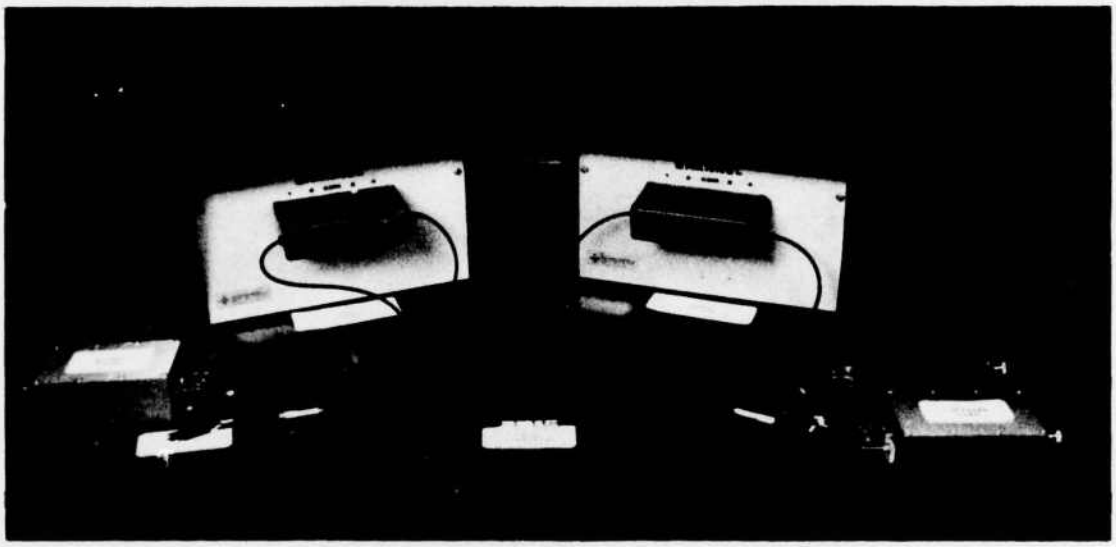

FIG. 47 Photograph of complete simulated optical multiplexed data link.

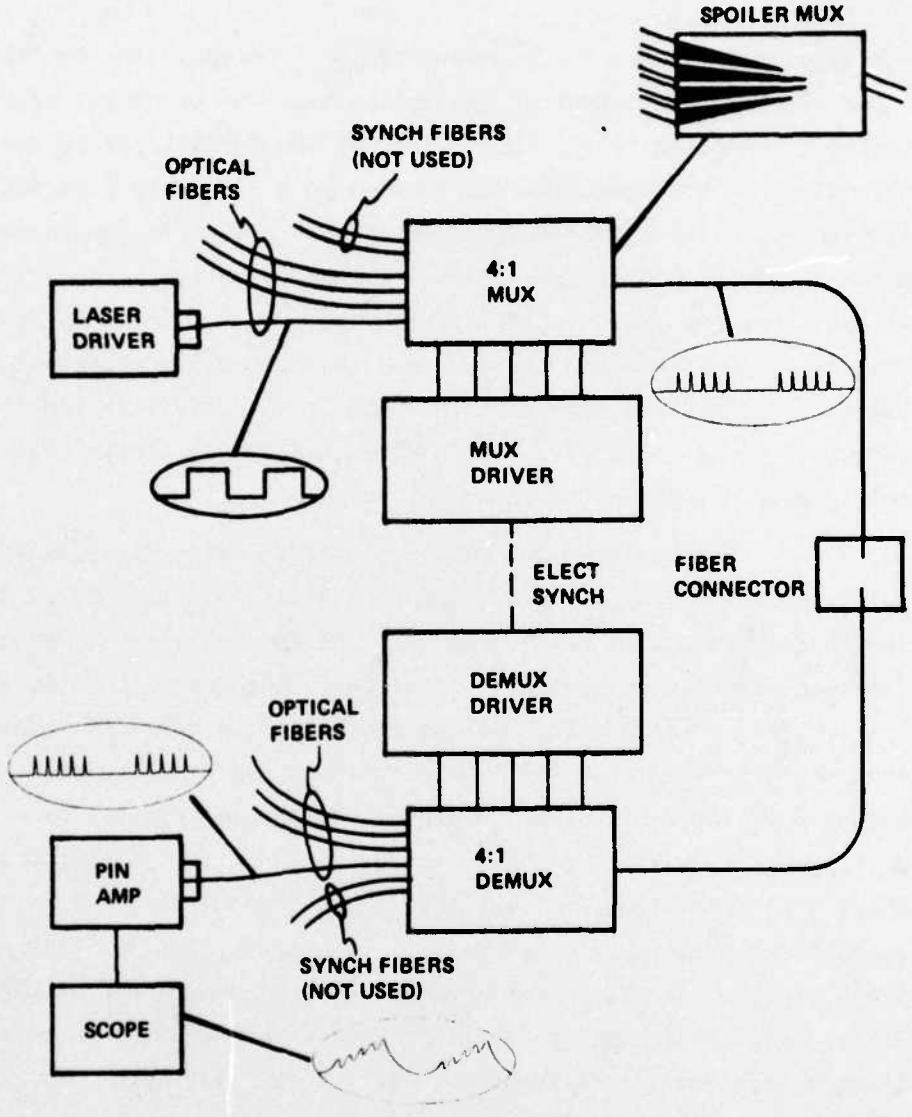

FIG. 48 Diagram of simulated optical multiplexed data link.

multiplexer unit, but the source could be coupled to any one of the four input fibers. The output of the multiplexer was connected by the fiber-to-fiber connector to the input fiber of the demultiplexer, and finally the output of the demultiplexer coupled to a PIN photodiode and associated electronics. The source was modulated with a 32 kb/s square wave, as before, and the multiplexer and demultiplexer driver sampled each channel at ten times per bit. Optical timing was not used for this demonstration but the synch fibers and the two separate drivers necessary to add optical timing in the future have been included in the demonstration link. For this test, an electrical line connected the demultiplexer driver with the multiplexer driver and provided the synchronization.

The complete link was tested first using dc voltages on the multiplexer and demultiplexer, and the results are summarized in Table 6. The throughput losses range from 27 to 31 dB for both devices and the fiber-to-fiber connector, while the signal to crosstalk ratio varies from 7 to 12 dB. There are two reasons for this wide range of signal to crosstalk ratio. Using both the multiplexer and the demultiplexer, the performance of the total link now depends on the performance of both devices Multiplexer 1, which was the first device packaged, generally yielded about 2 dB less signal to crosstalk ratio than Multiplexer 2. In addition, there is also the problem of unequal throughput loss for each channel when using the spoiler multiplexer design. Some channels are stronger than others, and the leakage crosstalk from a strong channel on to a weak channel is much more detrimental than for the reverse situation.

The results for the simulated link using the high frequency drivers are summarized in the photographs of Fig. 49. In this case, the bandwidth of the receiver is limited to about 50 kHz so that the partial reconstruction of the 32kb/s input square wave can be seen in the output waveforms. Figure 49(a) is for the source connected to input channel 1, (b) is for channel 2, etc. For this case the throughput loss was less than 30dB for all channels, and the signal to crosstalk ratio

OUTPUT FIBER	INPUT FIBER 1	INPUT FIBER 2	INPUT FIBER 3	INPUT FIBER 4
1	Through Loss 31 dB	S/C -10 dB	S/C -8 dB	S/C -12 dB
2	S/C -12 dB	Through Loss 29 dB	S/C -9 dB	S/C -11 dB
3	S/C -7 dB	S/C -11 dB	Through Loss 28 dB	S/C -12 dB
4	S/C -8 dB	S/C -9 dB	S/C -10 dB	Through Loss 27 dB

TABLE 6. Throughput loss and signal to crosstalk ratio for simulated link and dc voltages on mux and demux.

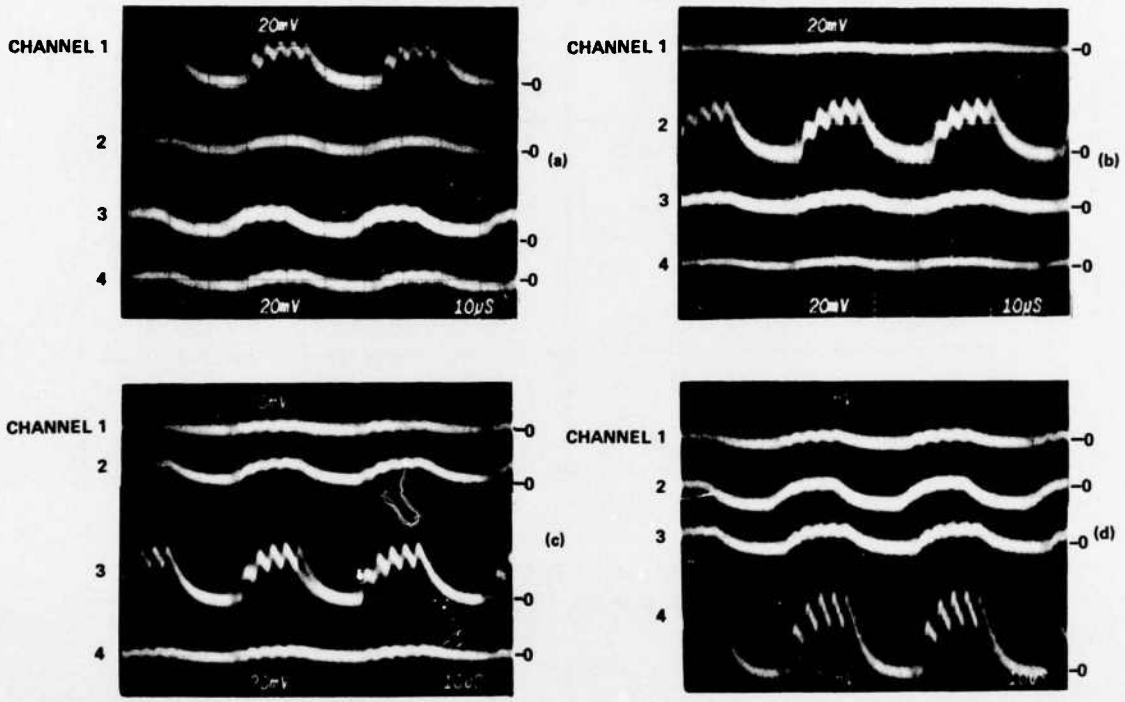

FIG. 49 (a) – (d) Optical output from demultiplexer using completed multiplexed data link. (a) through (d) are for input on channel 1 through 4, respectively.

varied from 4 to more than 10 dB. The exact cause of the deterioration of the worst case signal to crosstalk ratio is not known precisely at this time. Part of the problem is probably due to the slight overlap in driving pulses for different channels from the multiplexer and demultiplexer drivers. It was not possible with the present electronics to completely eliminate this overlap. Failure to completely turn a gate off before opening another gate could account for the observed crosstalk. Also, for this simulated link no adjustments were made for the optical transit time from the multiplexer to the demultiplexer, since timing was not incorporated. This transit time is only about 5nsec. but with the above-mentioned pulse overlap, this time delay could aggravate the problem further. Finally, there may exist some problems with the fast turn off of these devices due to charges accumlating in interface states and discharging at a relatively slow rate. This is a problem that needs further investigation.

8. SUMMARY AND RECOMMENDED RESEARCH

A 4:1 multiplexed optical data link has been constructed and tested. The functioning of the link centers on the performance of two identical electro-optic switching devices, a 4:1 multiplexer and a 4:1 demultiplexer. These devices are capable of handling the radiation from relatively large NA fibers and exhibit less than 15 dB throughput loss with an inherent signal to crosstalk ratio of 15 dB. Both devices have been packaged with permanently bonded butt coupled fibers. The final mux and demux units with multiple input and output fibers have less than 15 dB throughput loss with about 12 dB signal to crosstalk ratio.

The units have been assembled together and tested in an experimental data link. Electrical drivers were constructed for the mux and demux that enable the devices to sample each of four 32 kbit/s asynchronous data sources at the rate of ten times per bit. The information from the four channels would normally be combined on one optical fiber by the mux and separated at the demux end where the original

signal is recovered. The four channels were actually tested using one source and one detector to measure the throughput losses and signal to crosstalk ratio for each channel of the link. In general, the losses were less than 30 dB for both devices and the fiber to fiber coupler that connected them, and the signal to crosstalk ratio varied from 4 to more than 10 dB for the entire link.

The devices described here are capable of functioning in a practical optical data link if the proper optical sources are used. The multiplexer and demultiplexer loss is approximately 30 dB total so that if a 10 dB/km fiber is used, then a one km link will have a 40 dB loss. Used with a good Burrus-type LED capable of coupling several hundred μW into a single fiber, these devices and one km of optical fiber will yield a more than adequate S/N at the receiver end for the 32 kb/s data considered here. Longer links than one km or a faster data rate could be used with graded index fibers and higher power sources.

The results of this contract effort have shown that optical devices can be constructed to perform the switching and multiplexing functions required for a multiterminal link while using standard multimode fibers. This all-optical operation may avoid some of the complexity and expense that are inherent in converting signal from optical to electrical form for switching purposes and then back to optical form for transmission.

The most fruitful area for further research lies in modifying and improving the basic device performance by any one of a number of potential changes. As an example, it is possible to modify the present spoiler design so as to produce twice the index change with the same applied voltage. This is done by inserting additional electrodes adjacent to each of the main spoilers, as shown in Fig. 50, and connecting these "guard" electrodes with the opposite polarity voltage. The combination of negative spoiler electrodes and positive guard electrodes yields twice the relative index change for the same applied voltage.

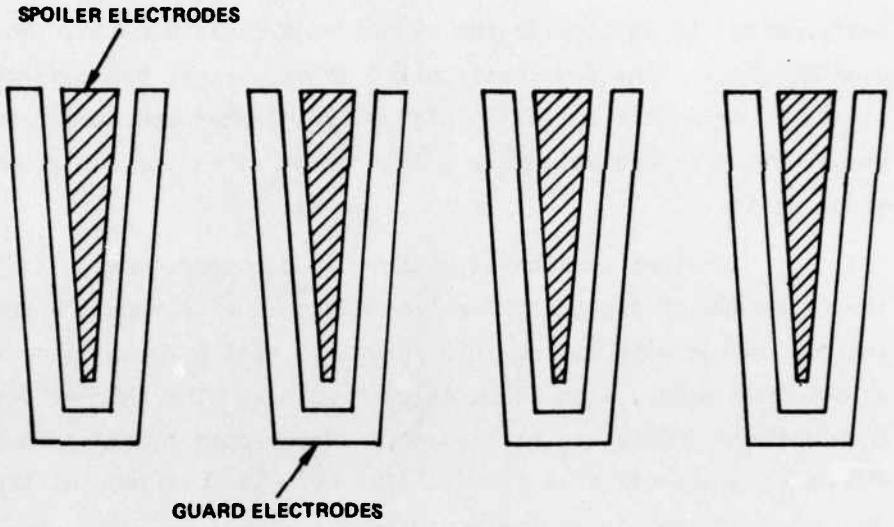

FIG. 50 Proposed spoiler mux electrode structure.

There are several ways this modification might be implemented. First, the present voltage could be cut in half and this would drop the power consumption by a factor of four and greatly reduce the electrical driving problems. The performance of the devices would remain the same, of course. Alternatively, the same voltage could be used and the device performance, in particular the signal to crosstalk ratio, should improve considerably. Some devices reported on earlier in our research have shown signal to crosstalk ratios as high as 20 dB when operated over an 800V range, which is equivalent to a 400V range using the new proposed electrode design.

Another possibility with this electrode design is to double the thickness of the crystal while holding the voltage the same as before. The new design with 150 μm thick crystals will give the same index change as obtained before with 75 μm thick crystals. The thicker crystals will enable these devices to be used with larger core fibers such as the 250 μm core plastic clad fibers. The obvious advantage of the 250 μm core fiber is that one may couple almost ten times the power coupled into a small core glass fiber when using less expensive and more reliable LED sources, and this clearly eases the device throughput loss problems. Another strong possibility is that the signal to crosstalk ratio of the multiplexer may improve considerably with the thicker crystals. The thin wafers of LT that are used at present tend to bend and deform easily under minor stresses, and this may be the cause for the imperfect light propagation. A 150 to 200 μm thick sample would be sturdier, easier to work with, and quite possibly devoid of the strains that scatter light. In particular, the thicker samples would not require the continuous support and protection with a crystal bond cement as is presently the case.

Some further effort may also be expended in improving the test demonstration link, such as including optical timing and synch pulses, by incorporating four Burrus-type LED sources, or by improving upon the

detection system. Also, improvements are desirable in the fiber-to-device bonding procedures described here. These bonding attempts were the first reported on for this kind of permanent, practical connection of fibers to an optical switching device. Improvements in procedure should lead to improved signal to crosstalk performance and more devices on a single crystal, such as a 12:3 multiplexer with integral fibers.

Other electrode designs and concepts are possible that improve, in additional ways, on the performance that has been obtained thus far. It is felt that further device research based upon these results will be able to increase the signal to crosstalk ratio, decrease the throughput losses, and lower the voltage and power requirements.

REFERENCES

1. A.R. Nelson, "Multiplexing and filtering of optical signals", Semiannual Technical Report ECOM - 1343 - 1, Army Contract No. DAABO7-76-C-1343; December 1976.

2. A.R. Nelson, D.H. McMahon and R.L. Grand, "Electro-optic channel modulator for multimode fibers," Appl. Phys. Lett., vol. 28, 321 (1976).

3. A.R. Nelson and D.H. McMahon, "Modulators for multimode single fiber communications systems," Electro-Optics/Laser 76 Conference Proc, New York, N.Y., Sept. 1976, paper II.4.

4. R.A. Soref, D.H. McMahon, and A.R. Nelson, "Multimode achromatic electro-optic waveguide switch for fiber optic communications," Appl. Phys. Lett., vol. 28, 716 (1976).

5. Handbook of Chemistry and Physics, Chemical Rubber Publishing Co., Cleveland, Ohio, 1961, page 3024.

6. S. Miyazawa, "Growth of $LiNbO_3$ single-crystal film for optical waveguides", Appl. Phys. Lett., vol. 23, 198 (1973).

7. Personal communication from Robert Carlson, Crystal Technology, Mountain View, CA.

REFERENCES (cont.)

8. Trademark of DuPont Chemical Company.

9. R.C. Kraguess and H.A. Waggener, U.S. Patent 3506509, 1970.

10. L.P. Boivin, "Thin film laser-to-fiber coupler", Appl. Opt., vol. 13, 391 (1974).

DISTRIBUTION LIST

101 DEFENSE DOCUMENTATION CENTER
ATTN: DDC-TCA
CAMERON STATION (BLDG5)
*012 ALEXANDRIA, VA 22314

103 CODE R123, TECH LIBRARY
DCA DEFENSE COMM ENGRG CTR
1860 WIEHLE AVE
001 RESTON, VA 22090

104 DEFENSE COMMUNICATIONS AGENCY
TECHNICAL LIBRARY CENTER
CODE 205 (P. A. TOLOVI)
001 WASHINGTON, DC 20305

200 OFFICE OF NAVAL RESEARCH
CODE 427
001 ARLINGTON, VA 22217

203 GIDEP ENGINEERING & SUPPORT DEPT
TE SECTION
PO BOX 398
001 NORCO, CA 91760

205 DIRECTOR
NAVAL RESEARCH LABORATORY
ATTN: CODE 2627
001 WASHINGTON, DC 20375

206 COMMANDER
NAVAL ELECTRONICS LABORATORY CENTER
ATTN: LIBRARY
001 SAN DIEGO, CA 92152

207 CDR, NAVAL SURFACE WEAPONS CENTER
WHITE OAK LABORATORY
ATTN: LIBRARY, CODE WX-21
001 SILVER SPRING, MD 20910

210 COMMANDANT, MARINE CORPS
HQ, US MARINE CORPS
ATTN: CODE LMC
002 WASHINGTON, DC 20380

211 HQ, US MARINE CORPS
ATTN: CODE INTS
001 WASHINGTON, DC 20380

212 COMMAND, CONTROL & COMMUNICATIONS DIV
DEVELOPMENT CENTER
MARINE CORPS DEVELOPMENT & EDUC COMD
001 QUANTICO, VA 22134

301 ROME AIR DEVELOPMENT CENTER
ATTN: DOCUMENTS LIBRARY (TILD)
001 GRIFFISS AFB, NY 13441

307 HQ ESD (DRI)
L. G. HANSCOM AFB
001 BEDFORD, MA 01731

314 HQ, AIR FORCE SYSTEMS COMMAND
ATTN: DLCA
ANDREWS AFB
001 WASHINGTON, DC 20331

403 CDR, US ARMY MISSILE COMMAND
REDSTONE SCIENTIFIC INFO CENTER
ATTN: CHIEF, DOCUMENT SECTION
002 REDSTONE ARSENAL, AL 35809

404 COMMANDER
US ARMY MISSILE COMMAND
ATTN: DRSMI-RE (MR. PITTMAN)
001 REDSTONE ARSENAL, AL 35809

405 COMMANDER
US ARMY AEROMEDICAL RESEARCH LAB
ATTN: LIBRARY
001 FORT RUCKER, AL 36362
Unclassified reports only.

406 COMMANDANT
US ARMY AVIATION CENTER
ATTN: ATZQ-D-MA
003 FORT RUCKER, AL 36362

407 DIRECTOR, BALLISTIC MISSILE DEFENCE
ADVANCED TECHNOLOGY CENTER
ATTN: ATC-R, PO BOX 1500
001 HUNTSVILLE, AL 35807

408 COMMANDANT
US ARMY MILITARY POLICE SCHOOL
ATTN: ATSJ-CD-M-C
003 FORT MCCLELLAN, AL 36201

417 COMMANDER
US ARMY INTELLIGENCE CENTER & SCHOOL
ATTN: ATSI-CD-MD
002 FORT HUACHUCA, AZ 85613

418 COMMANDER
HQ FORT HUACHUCA
ATTN: TECHNICAL REFERENCE DIV
001 FORT HUACHUCA, AZ 85613

419 COMMANDER
US ARMY ELECTRONIC PROVING GROUND
ATTN: STEEP-MT
002 FORT HUACHUCA, AZ 85613

420 COMMANDER
USASA TEST & EVALUATION CENTER
ATTN: IAD-CDR-T
001 FORT HUACHUCA, AZ 85613

421 COMMANDER
HQ US ARMY COMMUNICATIONS COMMAND
ATTN: CC-OPS-SM
001 FORT HUACHUCA, AZ 85613

437 DEPUTY FOR SCIENCE & TECHNOLOGY
OFFICE, ASSIST SEC ARMY (R&D)
001 WASHINGTON, DC 20310

438 HQDA(DAMA-ARP/DR. F. O. VERDERAME)
001 WASHINGTON, DC 20310

455 COMMANDANT
US ARMY SIGNAL SCHOOL
ATTN: ATSN-CTD-MS
001 FORT GORDON, GA 30905

470 DIRECTOR OF COMBAT DEVELOPMENTS
US ARMY ARMOR CENTER
ATTN: ATZK-CD-MS
002 FORT KNOX, KY 40121

473 COMMANDANT
US ARMY ORDNANCE SCHOOL
ATTN: ATSL-CD-OR
002 ABERDEEN PROVING GROUND, MD 21005

475 CDR, HARRY DIAMOND LABORATORIES
ATTN: LIBRARY
2800 POWDER MILL ROAD
001 ADELPHI, MD 20783

477 DIRECTOR
US ARMY BALLISTIC RESEARCH LABS
ATTN: DRXBR-LB
001 ABERDEEN PROVING GROUND, MD 21005

481 HARRY DIAMOND LABORATORIES, DEPT OF ARMY
ATTN: DRXDO-RCB (DR. J. NEMARICH)
2800 POWDER MILL ROAD
001 ADELPHI, MD 20783

482 DIRECTOR
US ARMY MATERIEL SYSTEMS ANALYSIS ACTY
ATTN: DRXSY-T
001 ABERDEEN PROVING GROUND, MD 21005

499 COMMANDER
US ARMY TANK-AUTOMOTIVE COMMAND
ATTN: DRDTA-RH
001 WARREN, MI 48090

507 COR, US ARMY AVIATION SYSTEMS COMMAND
ATTN: DRSAV-G
PO BOX 209
001 ST. LOUIS, MO 63166

511 COMMANDER, PICATINNY ARSENAL
ATTN: SARPA-FR-S
BLDG 350
002 DOVER, NJ 07801

512 COMMANDER
PICATINNY ARSENAL
ATTN: SARPA-ND-A-4 (BLDG 95)
001 DOVER, NJ 07801

513 COMMANDER
PICATINNY ARSENAL
ATTN: SARPA-TS-S #59
001 DOVER, NJ 07801

515 PROJECT MANAGER, REMBASS
ATTN: DRCPM-RBS
002 FORT MONMOUTH, NJ 07703

517 COMMANDER
US ARMY SATELLITE COMMUNICATIONS AGCY
ATTN: DRCPM-SC-3
002 FORT MONMOUTH, NJ 07703

518 TRI-TAC OFFICE
ATTN: CSS (DR. PRITCHARD)
001 FORT MONMOUTH, NJ 07703

531 CDR, US ARMY RESEARCH OFFICE
ATTN: DRXRO-IP
PO BOX 12211
001 RESEARCH TRIANGLE PARK, NC 07709

532 CDR, US ARMY RESEARCH OFFICE
ATTN: DRXRO-PH (DR. R. J. LONTZ)
PO BOX 12211
001 RESEARCH TRIANGLE PARK, NC 27709

533 COMMANDANT
US ARMY INST FOR MILITARY ASSISTANCE
ATTN: ATSU-CTD-MD
001 FORT BRAGG, NC 28307

537 CDR, US ARMY TROPIC TEST CENTER
ATTN: STETC-MD-A (TECH LIBRARY)
DRAWER 942
001 FORT CLAYTON, CANAL ZONE 09827

543 DIVISION CHIEF
METEOROLOGY DIVISION
COUNTERFIRE DEPARTMENT
002 FORT SILL, OK 73503

554 COMMANDANT
US ARMY AIR DEFENSE SCHOOL
ATTN: ATSA-CD-MC
001 FORT BLISS, TX 79916

555 COMMANDER
US ARMY NUCLEAR AGENCY
001 FORT BLISS, TX 79916

556 COMMANDER, HQ MASSTER
TECHNICAL INFORMATION CENTER
ATTN: MRS. RUTH REYNOLDS
001 FORT HOOD, TX 76544

563 COMMANDER, DARCOM
ATTN: DRCDE
5001 EISENHOWER AVE
001 ALEXANDRIA, VA 22333

564 CDR, US ARMY SECURITY AGENCY
ATTN: IARDA-IT
ARLINGTON HALL STATION
001 ARLINGTON, VA 22212

568 COMMANDER
US ARMY MOBILITY EQP RES & DEV CMD
ATTN: DRXFB-R
001 FORT BELVOIR, VA 22060

569 COMMANDER
US ARMY ENGINEER TOPOGRAPHIC LABS
ATTN: ETL-TD-EA
001 FORT BELVOIR, VA 22060

572 COMMANDER
US ARMY LOGISTICS CENTER
ATTN: ATCL-MC
002 FORT LEE, VA 22801

602 DIRECTOR, NIGHT VISION LABORATORY
US ARMY ELECTRONICS COMMAND
ATTN: DRSEL-NV-D
001 FORT BELVOIR, VA 22060

603 COR/OIR, ATMOSPHERIC SCIENCES LABORATORY
US ARMY ELECTRONICS COMMAND
ATTN: ORSEL-BL-SY-S
001 WHITE SANDS MISSILE RANGE, NM 88002

604 CHIEF
OFC OF MISSILE ELECTRONIC WARFARE
ELECTRONIC WARFARE LAB, ECOM
001 WHITE SANDS MISSILE RANGE, NM 88002

606 CHIEF
INTEL MATERIEL DEV & SUPPORT OFC
ELECTRONIC WARFARE LAB, ECOM
001 FORT MEADE, MD 20755

680 COMMANDER
US ARMY ELECTRONICS COMMAND
000 FORT MONMOUTH, NJ 07703

1 DRSEL-PL-ST
1 DRSEL-NL-D
1 DRSEL-WL-D
1 DRSEL-VL-D
3 DRSEL-CT-D
1 DRSEL-BL-D
2 DRSEL-NL-RM
1 DRSEL-TL-DT
*3 DRSEL-TL-MD
1 DRSEL-TL-M (Ofc of Record)
1 DRSEL-TE
1 DRSEL-MA-MP
**2 DRSEL-MS-TI
1 DRSEL-GG-TD
1 DRSEL-PP-I-PI
1 DRSEL-GS-H
1 DRSEL-CG (Mr. Doxey)
2 DRSEL-PA
1 DRSEL-RD
1 DRSEL-TL-D
1 USMC-LNO
1 TRADOC-LNO
25 Originating Office

700 CINDAS
PURDUE INDUSTRIAL RESEARCH PARK
2595 YEAGER ROAD
001 W. LAFAYETTE, IN 47096

701 MIT - LINCOLN LABORATORY
ATTN: LIBRARY (RM A-082)
PO BOX 73
002 LEXINGTON, MA 02173

703 NASA SCIENTIFIC & TECH INFO FACILITY
BALTIMORE/WASHINGTON INTL AIRPORT
001 PO BOX 8757, MD 21240

* Or number specified in contract. Add CORR's mail symbol.

** Unclassified reports only.

AD-A047 224 SPERRY RESEARCH CENTER SUDBURY MASS F/G 20/6
MULTIPLEXING AND FILTERING OF OPTICAL SIGNALS.(U)
JUN 77 A R NELSON DAAB07-76-C-1343
UNCLASSIFIED SCRC-CR-77-40 ECOM-1343-F NL

2 OF 2
AD
A047224

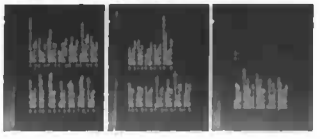

END
DATE
FILMED
1 -78
DDC

704 NATIONAL BUREAU OF STANDARDS
BLDG 225, RM A-331
ATTN: MR. LEEDY
001 WASHINGTON, DC 20231

705 ADVISORY GROUP ON ELECTRON DEVICES
201 VARICK STREET, 9TH FLOOR
002 NEW YORK, NY 10014

706 ADVISORY GROUP ON ELECTRON DEVICES
ATTN: SECY, WORKING GROUP D (LASERS)
201 VARICK STREET
002 NEW YORK, NY 10014

707 TACTEC
BATTELLE MEMORIAL INSTITUTE
505 KING AVENUE
001 COLUMBUS, OH 43201

709 PLASTICS TECH EVAL CENTER
PICATINNY ARSENAL, BLDG 176
ATTN: MR. A. N. ANZALONE
001 DOVER, NJ 07801

710 KETRON, INC.
ATTN: MR. FREDERICK LEUPPERT
1400 WILSON BLVD, ARCHITECT BLDG
002 ARLINGTON, VA 22209

711 METALS AND CERAMICS INF CENTER
BATTELLE
505 KING AVENUE
001 COLUMBUS, OH 43201

704 Westinghouse Defense and Electronic System Center
P.O.Box 746
Baltimore, MD 21203
001 ATT: Mr. L. F. Campbell

705 Bell Telephone Laboratories
Crawford Hill
Holmdel, NJ
001 ATTN: Dr. P. Kaiser

706 Carnegie-Mellon University
Department of Electrical Engineering
Schenley Park
Pittsburgh, PA 15213
001 ATTN: Prof. C. Tsai

707 Collins Radio
1200 N. Alma
Richardson, TX 75081
ATTN: Mr. Robert Hoss
001 Mail Stop: 401-134

708 US Dept of Commerce
Office of Telecommunications
325 South Broadway
Boulder, CO 80302
001 ATTN: Dr. R. L. Gallawa

709 Commander
US Army Foreign Science & Technology Center
220 Seventh St., NE
Charlottesville, VA 22901
001 ATTN: Dr. J. Galdo (DRXST-SD1)

710 Hughes Research Laboratories
3011 Malibu Canyon Rd.
Malibu, CA 90265
001 ATTN: Dr. M. Barnoski

711 Harris Electronics Systems
Melbourne, FL 32901
001 ATTN: Dr. E. Young

712 Honeywell, Inc.
574 Springfield Avenue
Westfield, NJ 07090
001 ATTN: Mr. T. Russell

713 IIT Research Institute
10 West 35th St.
Chicago, IL 60616
001 ATTN: Dr. N. Murarka

714 ITT
Electro-Optical Products Division
Box 7065
Roanoke, VA 24019
001 ATTN: Dr. J. E. Goell

715 RCA Laboratories
David Sarnoff Research Center
Princeton, NJ 08540
001 ATTN: Dr. J. Hammer

716 Defense & Space Systems Group of TRW
1 Space Park
Redondo Beach, CA 90278
001 ATTN: Dr. R. S. Kagiwada

717 LTV Aerospace
Advanced Technology Center
Dallas, TX 75222
001 ATTN: Dr. R. B. Hemphill

718 Corning Glass Works
Sullivan Park
Corning, NY 14830
001 ATTN: Mr. W. B. Bielawski

719 Bell Telephone Laboratories
600 Mountain Ave.
001 Murray Hill, NJ 07971

720 HQ ESD (DRI)
L. G. Hanscom AFB
Bedford, MA 01731
001 ATTN: Dr. Richard Payne

721 Grumman Aerospace Corp.
S. Oyster Bay Rd.
Bethpage, NY 11714
001 ATTN: Mr. David Ruppel

722 ITT Aerospace, Electronics, Components & Energy Group
ITT Defense Communications Division
492 River Road
Nutley, NJ 07110
001 ATTN: Dr. Peter D. Steensma

1. Commander — 3 copies
   US Army Electronics Command
   Fort Monmouth, NJ 07703
   ATTN: DRSEL-NL-MI

2. General Telephone & Electronics Corporation
   Electronics System Group
   Communications Systems Division
   ATTN: Dr. Harrington
   189 B Street
   Needham Heights, MA 02194

3. E. I. DuPont de Nemours & Company, Inc.
   PFX Fiber Optics Materials
   Research & Development Division
   Wilmington, DE 19898
   ATTN: Dr. K. S. Kamm

4. IBM
   Thomas J. Watson Research Center
   P. O. Box 218
   Yorktown Heights, NY 10598
   ATTN: Dr. E. G. Lean

5. Westinghouse Electric Corporation
   Research & Development Center
   1310 Beulah Road
   Pittsburgh, PA 15235
   ATTN: K. B. Steinbruegge

END

DATE
FILMED

1-78

DDC